Agronomy Research **20**(3), 682–724, 2022
https://doi.org/10.15159/AR.22.062

Chlorophyll fluorescence induction method in assessing the efficiency of pre-sowing agro-technological construction of the oilseed radish (*Raphanus sativus* L. var. *oleiformis* Pers.) agrocenosis

Y. Tsytsiura*

Vinnytsia National Agrarian University, Faculty of Agronomy and Forestry, Sonyachna Str., 3, UA21008 Vinnytsia, Ukraine
*Correspondence: yaroslavtsytsyura@ukr.net, yaroslav301974@gmail.com

Received: June 6th, 2022; Accepted: September 4th, 2022; Published: September 13th, 2022

Abstract. Chlorophyll fluorescence induction (CFI) is a measure of photosynthetic performance and is widely used by plant physiologists and ecophysiologists. The basic principle of CFI analysis is relatively straightforward. The specified method of analysis during 2015–2020 was applied to assess the optimality of selection of technological sowing parameters such as sowing rate (estimated interval 0.5–4.0 million germinable seeds ha^{-1}), row width (15–30 cm), pre-sowing fertilizer ($N_{0–90}P_{0–90}K_{0–90}$) for three varieties of oilseed radish. The widely tested basic indicators of the CFI curve (F_0, F_{pl}, F_m, F_{st}) were used, as well as possible indices and ratios calculated on their basis in accordance with the CFI analysis methodology.

For the first time, the species characteristics of oilseed radish were investigated by the nature of the CFI curve in relation to spring rape, white mustard, and spring mustard on the 1.5 germinable seeds ha^{-1} (30 cm row width, $N_0P_0K_0$) variant. It was established by the stress sensitivity category of the PSII photosystem that a reliable possibility of using the CFI method for identification studied technological options for sowing. The share of the influence of the technological factor of the sowing method (in %) on the formation of indicators F_0, F_{pl}, F_m, F_{st} in the dispersion scheme of the experiment was consistently 19.3, 8.4, 19.5, 6.3. The influence of the seeding rate factor on the results of F_0, F_{pl}, F_m, F_{st} was (in %) 26.6, 9.5, 42.3, 9.3 and the influence of the fertilizer factor was 13.5, 16.4, 5.7, 12.7, respectively.

The formation of the specified basic indicators of the CFI curve in the resulting interaction of the technological parameters of sowing depended on the hydrothermal conditions of the vegetation of oilseed radish with the share of influence of 20.1, 40.2, 28.1, 30.0, respectively. It was determined that the decrease in the indicator of the hydrothermal coefficient (in the ratio of the increase in the sum of average daily temperatures to the decrease in the amount of precipitation) ensures the following dynamics of changes in the main and derivative indicators of CFI: a decrease F_{pl} 1.3%, F_m 11.8%, ER 8.7%, Lwp 15.9%, R_{Fd} 25.3%, K_{prp} 21.9%, K_{fd} 17.7% and growth F_0 5.1%, F_{st} 7.3%, Q_{ue} 40.4%, K_{ef} 24.0%, V_t 71.3%.

The comparison during the study period of options 4.0 and 0.5 million germinable seeds ha^{-1} determined an averaged decrease in F_0 and F_{st} indicators by 29.5% and 29.1% while increasing F_{pl} and F_m by 2.2% and 38.5%. According to the determined level of CFI indicators for various technological schemes of sowing, an expedient option was recommended, which ensures the highest efficiency of the PSII photosystem of oilseed radish in the range of 1.0–2.0 germinable

seeds ha^{-1} with a fertilization rate of $N_{30–60}P_{30–60}K_{30–60}$ for row sowing and 1.5 germinable seeds ha^{-1} with a fertilization rate of $N_{60–90}P_{60–90}K_{60–90}$ for wide-row sowing.

Key words: chlorophyll fluorescence induction, fertilization rate, oilseed radish, row spacing, seeding rate, yield.

INTRODUCTION

Despite different approaches to the assessment of the physiological state of plants, the basic indicator of the state of plant life is the efficiency of the primary processes of photosynthetic reactions. The indisputable importance of this indicator is determined by both the importance of photosynthetic function in plant life and the high sensitivity of photosynthetic apparatus to changes in environmental factors, especially stress factors. On the other hand, any disruptions in the primary processes of photosynthesis directly affect changes in chlorophyll fluorescence and occur long before visible disturbances in the physiological state of plants, which can be assessed by obvious morphological changes in plant development, the rate of their growth processes and, ultimately, by the productivity level (Suárez et al., 2022).

It is an established fact that the source of fluorescence in the plant cell is light-absorbing pigment molecules, mainly chlorophyll (Kalaji et al., 2017a, 2017b). The effect of stressors of different nature on the plant is overwhelmingly related to the effect on the state of PSII reaction centers (RC), the S II antenna and the light-absorbing complex. The transfer of excitation energy of electrons between the pigments of these complexes and the glow of chlorophyll a reaction centers S II determine the induction curve of chlorophyll a fluorescence (Kalaji et al., 2017b). The shape of this curve is quite sensitive to the changes occurring in the photosynthetic apparatus of plants when adapting it to different environmental conditions, which was the basis for the wide use of the Kautsky effect in the study of plant photosynthesis and assessment of their condition under stress factors (Sloat et al., 2021). Certain interval segments of the chlorophyll fluorescence induction curve (CFI) can be used to analyze the physiological responses of the plant to stressful and induced-technological irritants. At the same time, the curve pattern varies depending on the intensity of exposure and the stress response of the plant itsel (Valcke, 2021).

According to a number of researchers, chlorophyll fluorescence is the fastest, most convenient and informative method among many other experimental methods used for ecological monitoring and assessment of the physiological condition of both individual plants and entire ecosystems (Cendrero-Mateo et al., 2019; Porcar-Castell et al., 2021; Schreiber & Klughammer, 2021).

Today, assessment of chlorophyll fluorescence parameters is used in models of crop productivity formation taking into account their phenotypic development and the corresponding system of successive critical periods of the vegetation (Souza & Yang, 2021), as well as in those that take into account trends in climate change and modern ideas about photosynthetic aspects of plant productivity in these conditions (Gensheimer et al., 2022).

Chlorophyll fluorescence indices are successfully used in assessing the overall stress tolerance of plants (Simeneh, 2020; Legendre et al., 2021; Oláh et al., 2021), plant reactions to heavy metals (Van Zelm et al., 2020; Javed et al., 2022), adaptive response to high and low temperatures (Cetner et al., 2017; Baldocchi et al., 2020; Kim et al.,

2021), drought, (Li et al., 2020; Kimm et al., 2021) etc. In recent years, it has been successfully used for early diagnosis of plant diseases and reaction to the degree of damage by pests and herbicides (Hupp et al., 2019; Amri et al., 2021; Sloat et al., 2021).

It also plays an important role in assessing soil nutrition of plants, its balance and efficiency in the formation of biomass and seeds (Larouk et al., 2021; Valcke, 2021).

Proved the possibility of applying the method of CFI as a criterion of optimality of agrotechnological formation of agrocenosis of field crops, especially against the background of different fertilization options (Herritt et al., 2021; Guo et al., 2022).

In addition to this oilseed radish has a wide range of uses in world practice which can be widely used from greening manure and sederation (Tsytsiura, 2019; Ferreira et al., 2021) to biofuel production (Kaletnik et al., 2020, 2021) but there is a lack of study of chlorophyll fluorescence aspects compared to white mustard, spring and winter rape.

Given the above facts, our research hypothesis was to clarify the effectiveness of the CFI method in determining the optimality of pre-sowing design of oilseed radish agrocenosis in the interrelated system of parameters density of standing - row width - level of mineral fertilizer (parameters of pre-sowing agro-technological construction) under the influence of appropriate hydrothermal conditions of its vegetation.

MATERIALS AND METHODS

Experimental conditions

The study of the functioning of the photosystem of oilseed radish plants depending on technological and agroecological factors was carried out during 2015–2020 on the research field (arranged by coordinates N 49°11′31″, E 28°22′16″) located in the zone of the Right-bank Forest-Steppe of Ukraine. The soil cover of the research field is represented by gray forest soils (Luvic Greyic Phaeozem soils (IUSS Working Group WRB, 2015)) with the following agrochemical parameters (for the period of crop rotation): humus 2.02–3.20%, mobile forms of nitrogen 67–92 mg kg^{-1}, phosphorus 149–220 mg kg^{-1}, potassium 92–126 mg kg^{-1} with metabolic acidity of soil solution (pH_{kcl}) 5.5–6.0.

The research scheme provided for the use of the spectrum of pre-sowing construction of oilseed radish agrocenosis was presented in a earlier publications (Table 1, Experiment 1). The applied scheme is described by Snedecor (1989) for studying the reaction of plants to a change in the configuration of its individual nutrition area (used by Ukrainian scientists in many studies as the Sinyagin's scheme (Sinyagin, 1975)). In this scheme the seeding rate (according to the indicator of the total number of plants m^{-2}) and the sowing method (as a criterion for the configuration of the nutrition area and the concretion of plants in the inter-row zone) are separately considered as a factor in the system of ANOVA analysis. Such a dispersion system allows analyzing the impact of sowing rates on the formation of certain indicators by means of a separate analysis based on the configuration of the nutrition area of one plant within the limits of the applied sowing scheme.

For study the peculiarities of the CFI curve formation in comparison with other cruciferous crops, a small plot experiment was carried out (Table 1, Experiment 2) To comply with the rule of uniform abolition, all crops were sown at same time with the same technological variantat (1.5 million pcs. ha^{-1}, inter-row 30 cm, $N_0P_0K_0$). This variant used for all crops in agronomic practice of the research region. All other components of the cultivation technology of the selected group of cruciferous crops were the same.

Table 1. Agrotechnological variants of oilseed radish agrocenosis construction were used in the experiment (Tsytsiura, Ya.H. 2021)

Experiment 1. Specific characteristics CFI of oilseed radish in relation to other cruciferous crops		
Year conditions in the year data expression	Cruciferous crops	Scheme of combinations of variants
Year conditions in the year data expression: 2015–A_1, 2016–A_2, 2017–A_3, 2018–A_4, 2019–A_5, 2020–A_6		
2015–A_1, 2016–A_2, 2016–A_3, 2016–A_4, 2016–A_5, 2016–A_6,	Oilseed radish *(Raphanus sativus* L. var. *oleiformis* Pers.) (B_1) White mustard *(Sinapis alba* L.) (B_2) Spring rape (*Brassica napus* L. var. *oleifera* Metzg.) (B_3) Spring bittercress (*Brassica campestris* var. *oleifera* f. *annua* D.C.) (B_4)	$A_{1–6} \times B_{1–4}$

Experiment 2. Formation of CFI indicators depending on pre-sowing agro-technological construction of the oilseed radish agrocenosis		
Plant placement due to the ratio of the sowing rate (factor B – million germinable seeds ha^{-1}) to the sowing method (factor C – row method (15 cm), wide-row method (30 cm))		Rate of fertilizations (facor D), $kg \cdot ha^{-1}$
4.0 (1.67 (B_1) × 15 (C_1))	2.0 (6.67 (B_1) × 30 (C_2))	$N_0P_0K_0$ (D_1)
3.0 (2.22 (B_2) × 15 (C_1))	1.5 (3.33 (B_2) × 30 (C_2))	$N_{30}P_{30}K_{30}$ (D_2)
2.0 (3.33 (B_3) × 15 (C_1))	1.0 (2.22 (B_3) × 30 (C_2))	$N_{60}P_{60}K_{60}$ (D_3)
1.0 (*6.67 (B_4) × **15 (C_1))	0.5 (1.67 (B_4) × 30 (C_2))	$N_{90}P_{90}K_{90}$ (D_4)
Year conditions in the year data expression: 2015–A_1, 2016–A_2, 2017–A_3, 2018–A_4, 2019–A_5, 2020–A_6		
Scheme of combinations of variants	$A_{1–6} \times B_{1–4} \times D_{1–4}$	The total number of combinations (N = 192)

* – distance in a row, cm; ** – width of the row, cm.

Weather conditions

The temperature regime and the humidification regime for the period of research for the stage of formation of oilseed radish yield had significant differences (Fig. 1, Table 2). This allowed to analyze the features of the functioning of the plant photosystem from the standpoint of fluorescence of chlorophyll induction not only in view of agrotechnological variants of agrocenosis, but also from the standpoint of abiotic (agroecological) factors. In particular, the weather conditions in 2015 and 2018 were the most stressful in terms of the impact on plant growth processes and the formation of its assimilation surface in accordance with the values of the hydrothermal coefficient. At the same time, according to the intensity of the increase in average daily temperatures in the absence of atmospheric moisture (Fig. 1) in some years of research, the conditions of 2015 should be considered the most stressful from the standpoint of direct impact from the phenological phase of budding and flowering (Biologische Bundesanstalt, Bundessortenamt and CHemical industry (Test Guidelines…, 2017) (BBCH) 38-64). That is why the accounting indicators of the 2015 experiment were used to detail the effect of temperature and humidity on the induction of chlorophyll fluorescence.

According to the presented data of the stress effect on the growth processes of oilseed radish plants for years of observation 2015–2020 can be placed in the next decrease row 2018–2015–2017–2016–2019–2020.

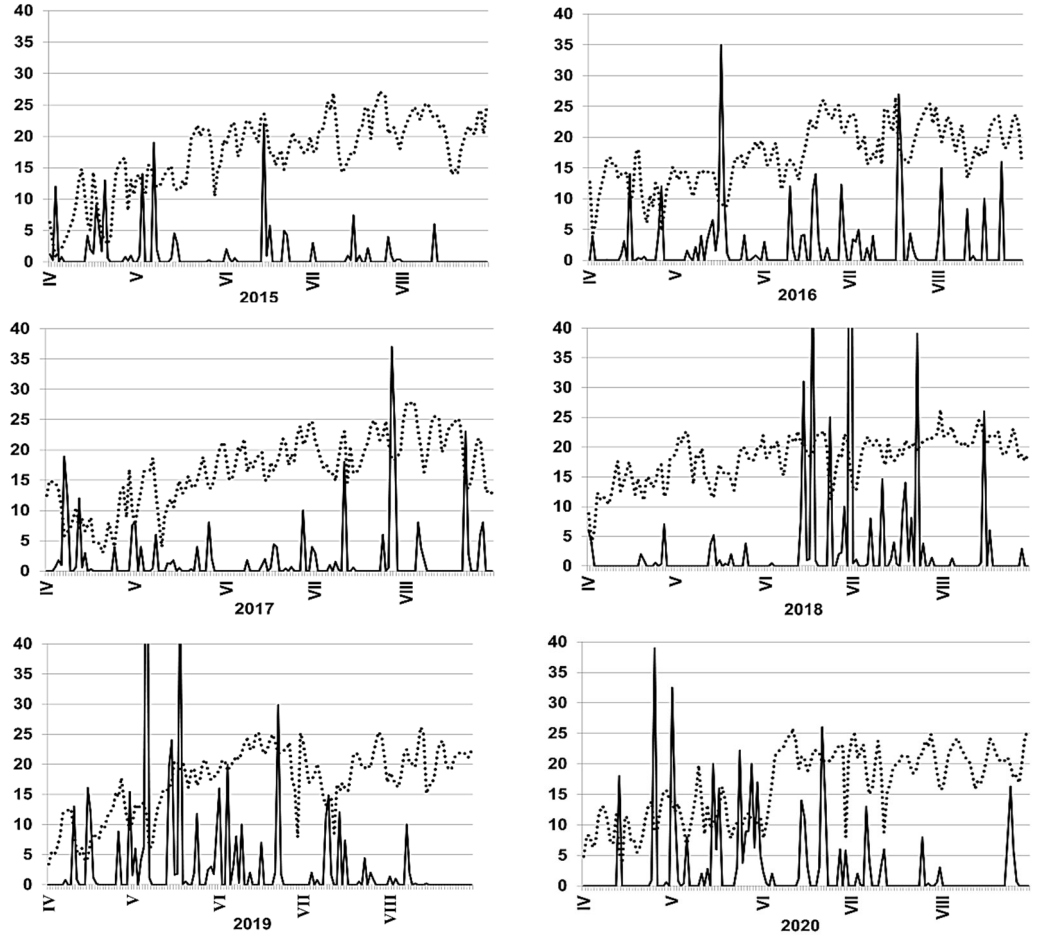

Figure 1. Daily total rainfall and average air temperature during spring triticale growing season, 2015–2020 (dotted line – average daily temperature, °C, continuous line – rainfall, mm) (with added data based Tsytsiura, 2020).

Table 2. Hydrothermal coefficient* for the growing season of oilseed radish (monthly), 2015–2020 (with added data based Tsytsiura, 2020 a)

Year of research	Months					On average for the growing season
	V	VI	VII	VIII	IX	
2015	0.719	0.613	0.230	0.061	0.684	0.430
2016	1.227	0.893	0.682	0.486	0.063	0.663
2017	0.645	0.349	0.806	0.563	1.983	0.824
2018	0.258	3.124	1.349	0.349	0.680	1.179
2019	4.710	1.555	1.003	0.235	0.945	1.690
2020	5.489	1.474	0.649	0.474	1.208	1.859

* – $HTC = \sum R \times (0.1 \times \sum t_{>10})^{-1}$, where the amount of precipitation (ΣR) in mm over a period with temperatures above 10 °C, the sum of effective temperatures (Σt > 10 °C) over the same period, decreased by a factor of 10 (Selyaninov, 1928). Ranking of values: HTC > 1.6 – excessive humidity, HTC 1.3–1.6 – humid conditions, HTC 1.0–1.3 – slightly arid conditions, HTC 0.7–1.0 – arid conditions, HTC 0.4–0.7 – very arid conditions (ranking on the basis: Selyaninov, 1928; Evarte-Bundere & Evarts-Bunders, 2012).

Chlorophyll fluorescence induction method

It was used to measure the parameters of chlorophyll flowering a portable fluorometer 'Floratest'. This fluorometer developed by the scientific and engineering center of microelectronics of the Glushkov Institute of Cybernetics (Romanov et al., 2011). The device is equipped with an LCD screen (128×64 pixels) and a remote optoelectronic sensor with an irradiation wavelength of 470 ± 15 Nm, a spot irradiation area of at least 15 mm^2 and an irradiance within it of at least 2.4 Wm^{-2} (Fig. 2). The spectral range of fluorescence intensity measurements ranges from 670 to 800 nm. The software provided with the device (Portable fluorometer …, 2011). The measurement duration was 4 minutes, the functional period of measurement was 3 minutes.

For measurements, has been used the plant leaf on the phase of the beginning of flowering (BBCH 61-63) from the middle tier by plant height in each series of experiments in the number of 25 for each repetition. Plant leaf was placed in an optical block in the middle part with its upper side toward the light source in. Measurements were taken after leaf adaptation to darkness for 10 min in 4-fold replications for each variant at 90 points with time intervals from 3 microseconds to 300 seconds followed by calculation of relative units for 3 min with registration of changes in chlorophyll fluorescence. The initial measuring point for the 'Floratest' was 1 ms.

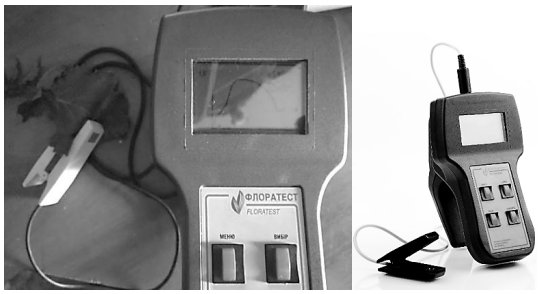

Figure 2. Portable fluorometer 'Floratest' (left) and chlorophyll fluorescence measurements process on oilseed radish leaves (laboratory cultivation).

The measurements were based on the chlorophyll fluorescence induction curve values (Kautsky effect) (Fig. 3) obtained on native leaves.

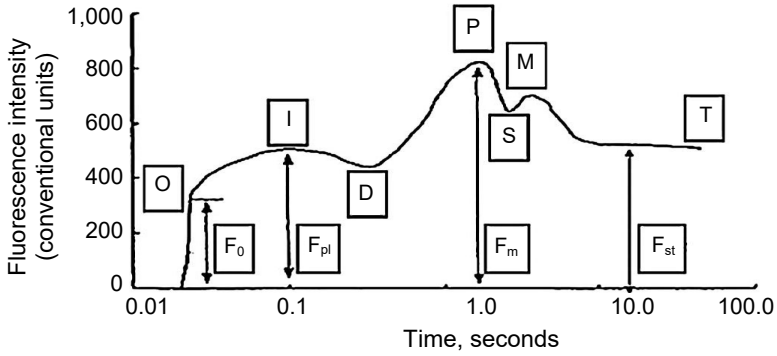

Figure 3. A typical chlorophyll fluorescence induction (CFI) curve (Kautsky curve) (vertical axis – fluorescence intensity (relative units), horizontal axis – time (c)) (Brestic & Zivcak, 2013).

Calculated indicators and statistical analysis

During the experiments, we analyzed the commonly used indices of the curve (Brestic & Zivcak, 2013; Kalaji et al., 2014, 2017a, 2017b), such as:

F_0 – minimal fluorescence (dark) – fluorescence intensity with all PS II reaction centers open while the photosynthetic membrane is in the non-energized state, i.e., dark or low light adapted (O level in the O-I-D-P-T CFI curve);

F_{pl} – value of the 'plateau' fluorescence induction for the time of reaching a temporary slowing down of its signal growth I level in the O-I-D-P-T CFI curve);

F_m – maximal fluorescence (after dark adaptation) – fluorescence intensity with all PSII reaction centers closed all nonphotochemical quenching processes are at a minimum (P level in the O-I-D-P-T CFI curve);

F_{st} – fluorescence in steady state (T level in O–I–D–P–T CFI curve). This is the stationary value of fluorescence induction after the light adaptation of the plant leaf (in our case, its stationary level after 3 min after the start of illumination).

The following parameters were calculated using the standardized CFI curve analysis protocol (Brestic & Zivcak, 2013):

– fluorescence rise according to formula 1:

$$dF_{pl} = F_{pl} - F_0 \tag{1}$$

– maximum variable fluorescence according to formula 2:

$$F_v = F_m - F_0 \tag{2}$$

– index of the effect of exogenous and endogenous factors on the relative number of inactive reaction centers according to formula 3 (Brion et al., 2000; Stirbet & Govindjee, 2011):

$$\frac{dF_{pl}}{F_v} \tag{3}$$

It is also used as an indicator of plant condition regarding the presence of possible phytopathogenic infection, provided this indicator ≥ 0.4–0.5 indicates the presence of infection and significantly increases the probability of detecting viral lesions compared to visual observation (Sarahan, 2011).

– photochemical efficiency or quantum efficiency (EP) according to formula 4, which is an indicator of the impact of exogenous factors and depends on the efficiency of the photochemical reactions of the photosynthetic system II (PS II):

$$EP = \frac{F_v}{F_m} \tag{4}$$

– photochemical quenching (Que) according to formula 5 (Larouk et al., 2021):

$$Q_{ue} = \frac{F_0}{F_v} \tag{5}$$

Leaf water potential (L_{wp}) according to formula 6 (Larouk et al., 2021):

$$L_{wp} = \frac{F_m}{F_0} \tag{6}$$

– plant viability index (according to formula 7), which measures the photosystem II photochemistry efficiency, PS II, and determines the fraction of light absorbed by chlorophyll bound to PS II (photosystem II). It can provide a measure of the rate of linear

electron transport and consequently the value of total photosynthesis (Korneev, 2002; Lichtenthaler et al., 2005: Stirbet & Govindjee, 2012; Murchie et al., 2018).

$$RF_d = \frac{F_m - F_{st}}{F_{st}} \quad (7)$$

– indicator of endogenous (stress) factors according to formula 8:

$$K_{ef} = \frac{F_{st}}{F_m} \quad (8)$$

– value of photochemical quenching of fluorescence according to formula 9:

$$QP = \frac{F_m - F_{st}}{F_m - F_0} \quad (9)$$

QP value is affected by both photochemical (CO_2 fixation) and non-photochemical processes (thermal dissipation of energy of the excited state of chlorophyll molecules), – characterizes the adaptability of plants to environmental conditions (Korneev, 2002; Goltsev et al., 2014).

– index of the efficiency of the primary reactions of photosynthesis according to formula 10:

$$K_{prp} = \frac{F_v}{F_0} \quad (10)$$

– fluorescence decay coefficient according to formula 11:

$$K_{fd} = \frac{F_m}{F_{st}} \quad (11)$$

– relative change of fluorescence at time t according to formula 12:

$$V_t = \frac{F_{st} - F_0}{F_m - F_0} \quad (12)$$

To compare the parameters we used a relative value of comparison (%) – the ratio of absolute indicators relating to different objects, but to the same time, calculated according to formula 13 (Rumsey, 2016):

$$k_{\text{comparison}} = \frac{k_1}{k_2} \times 100 \quad (13)$$

where k_1 – indicator of the first object under study, k_2 – indicator of the second object under study.

The seed yield was considered in the format of its biological level by accounting and subsequent calculation of the average seed yield from one plant (in grams) from the general population of plants consisting in the CFI curve indicators accounting.

The studies used varieties (‘Zhuravka’, ‘Raiduha’, ‘Lybid’) of oilseed radish. Given the similarity of the results obtained for the studied of this varieties in the tables and graphics presented only data on the variety ‘Zhuravka’.

The data obtained were analyzed using the analysis of variance (ANOVA) and the GLM procedure. Tukey HSD Test in R (version R statistic i386 3.5.3) was also used. Multiple comparisons of the parameter means computed were performed using the smallest significant difference *LSD* at 5% (95% family-wise confidence level for Tukey HSD Test) for all the parameters studied. Correlation and regression analyzes were performed according to the generally accepted scheme with the statistical software Statistica 10 (StatSoft – Dell Software Company, USA).

RESULTS AND DISCUSSION

Experiment 1. Specific characteristics CFI of oilseed radish in relation to other cruciferous crops

In order to consider the peculiarities of the formation of the basic and calculated indicators indicators of the chlorophyll fluorescence induction curve (CFI) in oilseed radish plants were additionally compared for three species of cruciferous crops, which are widely used in agricultural practice. During the 2015–2020 period of comparative study, a number of significant differences were established in the indicated parameters in oilsed radish (Table 3, Fig. 4).

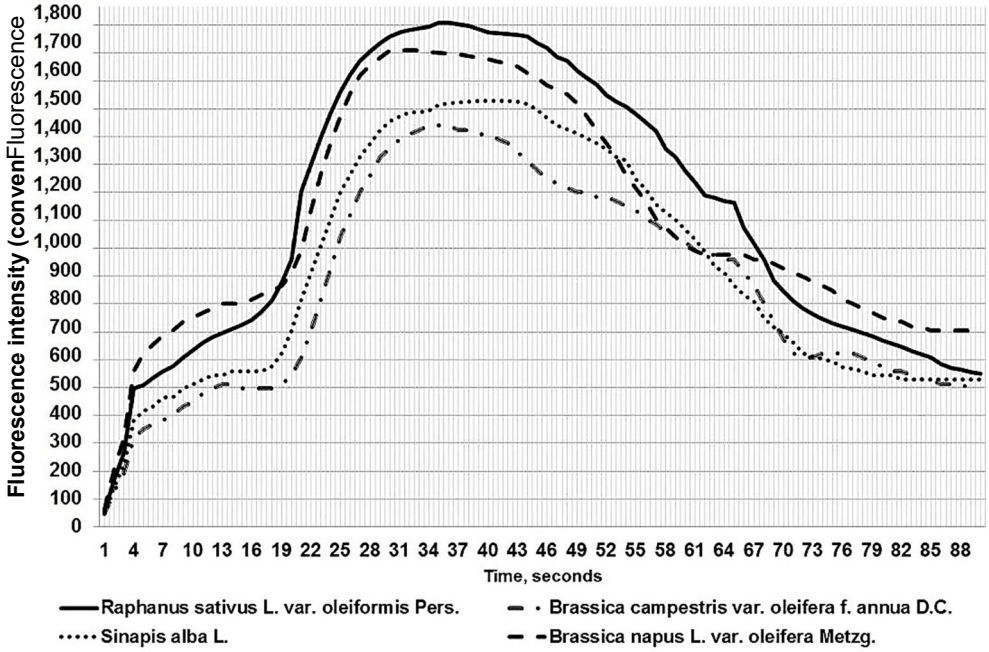

Figure 4. Comparison of CFI curve for four species of cruciferous plants, average average data 2015–2020.

The level of initial fluorescence after dark adaptation F_0 in oilseed radish plants when comparing the average values, was 29.7% higher than in white mustard (*Sinapis alba* L.) and 55.6% higher than in spring bittercress (*Brassica campestris* var. *oleifera* f. *annua* D.C.), however, it is 12.4% lower than that of spring rape (*Brassica napus* L. var. *oleifera* Metzg.).

Such data indicate a specific feature of the transfer of excitation energy from the antenna to the reaction center of the PSII photosystem and the different efficiency of such transfer according to the ergocapacitance indicators of the process. In oilseed radish plants, based on the studies of Kalaji et al. (2016, 2017), Baker & Rosenqvist (2020), Ashrostaghi et al. (2022), the excitation energy transfer system between the pigment molecules of the light-gathering antenna of the PSII cenrer has a high initiation threshold.

Table 3. Basic and calculated values of the CFI curve in selected cruciferous species (relative units of the fluorescence reference for the phase of full flowering of plant species BBCH 65–67), 2015–2020

Plant species	Basic indicators				Estimated indicators and indices											
	F_0	F_{pl}	F_m	F_{st}	dF_{pl}	F_v	dF_{pl}/F_v	EP	L_{wp}	Q_{ue}	RF_d	K_{ef}	QP	K_{prp}	K_{fd}	V_t
Raphanus sativus L. var. oleiformis Pers.	498 ± 56	671 ± 74	1,808 ± 509	551 ± 124	173	1,310	0.132	0.725	3.631	0.380	2.281	0.305	0.960	2.631	3.281	0.040
Brassica campestris var. *oleifera* f. *annua* D.C.	320 ± 42	512 ± 97	1,440 ± 308	496 ± 87	192	1,120	0.171	0.778	4.500	0.286	1.903	0.344	0.843	3.500	2.903	0.157
Sinapis alba L.	384 ± 53	560 ± 114	1,529 ± 314	528 ± 94	176	1,145	0.154	0.749	3.982	0.335	1.896	0.345	0.874	2.982	2.896	0.126
Brassica napus L. var. *oleifera* Metzg.	560 ± 64	800 ± 67	1,711 ± 439	688 ± 122	240	1,151	0.209	0.673	3.055	0.487	1.487	0.402	0.889	2.055	2.487	0.111

$LSD_{0.5}$	F_0	F_{pl}	F_m	F_{st}
$LSD_{0.5}$ factor A (year)	8.51	7.67	6.50	5.91
$LSD_{0.5}$ factor B (plant species)	7.57	6.38	5.82	4.84
$LSD_{0.5}$ interaction AB	10.80	11.38	9.59	8.77

The share of influence of experimental factors				
factors	F_0	F_{pl}	F_m	F_{st}
A	19.832	25.862	26.324	28.639
B	51.321	47.369	53.437	48.251
AB	28.847	26.769	20.239	23.110

Thus, this is a sign of its stress sensitivity to high and, especially, excessive thickening. It will show a sensitive response to a smaller range of densities than for a species with a low F_0 value, for example, *Brassica campestris* var. *oleifera* f. annua D.C. It is predicted that the reduction of the nutrition area of one plant in oilseed radish will give a more noticeable reaction in the change of the fluorescence induction of chlorophyll than in spring bittercress and white mustard. However, oilseed radish will be more tolerant to changes in the nutrition area than spring rape. This is consistent with findings for other crops in similar studies (Gu et al., 2017; Shomali & Aliniaeifard, 2020; Hosseinzadeh et al., 2021). The conclusion is also consistent with the agrotechnological assessment of the cultivation of the main cruciferous crops and its reaction to changes in the density of placement (Shpaar, 2012; Kayaçetin, 2020).

A similar character was established for the formation of such an indicator as F_{pl} – the value of the fluorescence induction 'plateau'. For spring mustard and white mustard, its value was significantly lower compared to oilseed radish and spring rape. The maximum value of the indicator of 800 relative units of the fluorescence was noted in spring rapeseed (in total, it is 56.3% more than in spring bittercress, 42.9% than in white mustard, and 19.2% than in oilseed radish). For oilseed radish, there is also a pronounced arc-shaped transition from the maximum value of F_{pl} to the beginning of an intense increase in the induction of chlorophyll. The same character with a pronounced 'plateau' was also noted for spring bittercress and with a shift in fixing time for white mustard at the already mentioned lower amplitude. This type of fixation of the F_{pl} indicates differences in the functioning of the studied plant species. In oilseed radish, this confirms its sensitivity to changes in cenosis tension with changes in density, as well as to a possible reaction to changes in the concentration of chlorophyll in case of intensive densification. This is indicated by the findings in the studies and generalisations of Brack & Frank (1998), Brestič et al. (2012), Brestic & Zivcak (2013).

The F_m indicator also had species specificity. The F_m intensity of oilseed radish during the years of study was the highest among the studied species and amounted to 1,018 relative units. For example, this indicator in spring rape was 937 relative units, white mustard – 621, and in spring bittercress – 569. It is known that even with a saturating pulse, F_m depends on the chlorophyll content of the tissue (Brion et al., 2000; Brestic & Zivcak, 2013; Herritt et al., 2020). A decrease in F_m indicates that the object of study is under stress, which means that not all of the PSII electron acceptors can be fully recovered. Considering that the basic stand density for the studied crucifer species of 1.5 million germinable seeds ha^{-1} is one of the recommended in the study area, we assumed about the different stages of physiological state of leaves of different crucifer species at the flowering stage (BBCH 65-67). Given that the studied species in order of prolongation of vegetation can be placed in the following order - spring bittercress - white mustard - spring rape - oilseed radish (Shpaar, 2012) and considering the physiological specificity of crucifers to the maximum reduction of the percentage of leafiness of the stem during plant maturation (Zhang et al., 2020), the indicator F_m indicates that the productive efficiency of the leaf photosystem of spring bittercress is phenostatically shifted to the phenological phase of stemming-budding. Due to this, the age of the leaf at the flowering stage is less than for oilseed radish and spring rape with an intensive peak value of the activity of the assimilation apparatus at the phenological phase of budding-beginning of flowering and a functionally longer period of vital activities of each leaf of plant. For white mustard, an intermediate pattern has been

established in the dates indicated. This is confirmed by the leaf water potential (L_{wp}), which is the ratio $F_m F_0^{-1}$. In healthy and young leaves, this ratio is about 4–5, and its value depends on the effect of certain stress factors on the plant, e.g. during drought the ratio can be reduced to 1 (Wang et al., 2016), indicating the destruction of PSII. This is confirmed by our data - the indicator L_{wp} decreases consistently in the row spring bittercress (4.50) - white mustard (3.98) - oilseed radish (3.63) - spring rape (3.05).

Numerous studies confirm that the EP parameter ($F_V F_m^{-1}$) measured in dark adapted plants reflects the potential quantum efficiency of PSII and can be used as a reliable indicator of photochemical activity of the photosynthetic apparatus. For most plants under full development under non-stress conditions the maximum value of this parameter is 0.830 (Björkman & Demmig, 1987; Brestic & Zivcak, 2013; Guidi et al., 2019).

Its decrease means that before the measurement, the plant was subjected to a stress that damaged the S function, resulting in a decrease in electron transport efficiency. This is often observed in plants exposed to various stress factors (Kalaji et al., 2017b; Petjukevics & Skute, 2022; Feria-Gómez et al., 2022). The change in EP parameter value is considered the most sensitive indicator of the effect of photo-inhibition (the phenomenon of suppression of photosynthesis and damage to the photosynthetic apparatus at high light intensity) (He et al., 1996). The EP parameter can also be used as an indicator of the degradation of D_1-protein (an important element of PSII), which has been damaged during stress, e.g., light stress, or modified for other reasons, leading to inactivation of FS reaction centres (Rintamäki et al., 1995). However, during prolonged stress, there is a significant reduction in EP, which is also accompanied by a decrease in photosynthetic intensity (Flexas e al., 2004; Posudin & Bogdasheva, 2010; Brestič et al., 2012; Brestic & Zivcak, 2013; Stirbe et al., 2014; Kalaji et al., 2017b; Keller et al., 2019; McAusland et al., 2019; Pérez-Bueno et al., 2019; Casto et al., 2021). Thus, taking into account that the EP is an effective indicator of the optimality of growth and physiological processes of plants associated with their photo-assimilating activity, the agro-technological parameters of 1.5 million pcs. ha^{-1} of germinable seeds on an unfertilized variant are the most optimal in such a reduction series of species - spring bittercress - white mustard - oilseed radish - spring rape. This is also indicated by other calculated coefficients of intensity and quality of chlorophyll fluorescence process, in particular Q_{ue}, R_{fd}, V_t.

It should be noted that a special area on the CFI curve in the period of 62–65 seconds of fixation of the device. This segment of the curve is noted in all years of research and well expressed in oilseed radish. According to Korneev (2002), such a transition on the segment of the F_m–F_{st} curve indicates physiological mechanisms of preadaptation of the PSII photosystem during the transition to stationary fluorescence. According to Flexas et al. (2002) this characterizes the stress sensitivity of the species in the area of transition from the active expression of maximum fluorescence to its stationary level. The low severity of this area on the CFI curve in white mustard is apparently due to the higher rate of physiological aging of leaves than in other cruciferous species in the analyzed group, as indicated in the publications Hasanuzzaman (2020).

In our study the parameter F_{st} should also be mentioned separately. This parameter characterises the total intensity of chlorophyll fluorescence emitted by photosynthetic objects under steady-state light conditions. After dark adaptation, it takes about 3–5 minutes for CFI curve to reach stationary state (F_{st} level). At this point, there is an equilibrium between the assimilative force production in photochemical reactions

(ATP and NADPH molecules) and the enzymatic reactions that use these molecules in the dark phase. Any disruption of photosynthetic reactions (e.g. caused by stress factors) delays reaching stationary state (F_{st}) (Korneev, 2002; Kalaji et al., 2017, 2017a). It is noted (Ruban & Murchie, 2012; Mathur et al., 2014; Magney et al., 2020) that under intensive stress as well as natural leaf ageing, the F_{st} value can be significantly higher than the initial F_0 value and vice versa under optimum conditions. Under excessive stress factor conditions, the time to reach F_{st} is intensively shortened compared to normal or optimum growth and development conditions for the plant species. The results of our studies in the case of the value of F_{st} for the studied plant species confirmed the findings regarding the phenostasis of leaf development and photosynthetic system of different cruciferous species at the flowering date, and also allow us to indicate the specificity of photosystems of oilseed radish and other studied species, for which the difference between F_0 and F_{st} parameters was 53 relative units, and for spring bittercress with a similar index this value was 176 relative units. Thus, leaf apparatus of oilseed radish is highly stress-sensitive due to the possibility of using the difference index F_0 and F_{st} to assess the overall level of adaptivity of the plant's photosystem. These conclusions are confirmed by similar studies on a number of other plant species (Liu et al., 2017; Baba et al., 2019; Maguire et al., 2020; Dechant et al., 2020).

Should also note that according to the value of photochemical quenching fluorescence (QP), which characterizes the overall adaptability of plants to environmental conditions (Korneev, 2002), the studied species according to their QP values can be placed in the following order: oilseed radish (0.960) - spring rape (0.889) - white mustard (0.874) - spring bittercress (0.843).

The species viability index (R_{Fd}), which, when applied to the calculated indexes of the CFI curve, shows the threshold level of the environmental stressor (Korneev, 2002; Gururani et al., 2015), this series has a different character according to our estimates: oilseed radish (0.695) - spring bittercress (0.656) - white mustard (0.655) - spring rape (0.598).

It can be stated, based on the analysis of the basic and derivative indices of the CFI curve, that oilseed radish has both a high level of adaptability and also capable of long-term resistance to high levels of exogenous stress factors, unlike spring rape, in which the adaptive potential has limitations relative to the level of stress factor value.

The adaptability of the species is also characterised by the relative fluorescence variable at time t - index V_t. According to received data, which are also confirmed by Brestic & Zivcak (2013), a lower level of V_t indicates that the photosynthetic and photochemical processes in the plants are optimal against the respective hydrothermal regimes of the environment, determining the smoothness of the threshold indicative points of the CFI curve. For oilseed radish in particular, this indicator was 69.5% lower than the average value for the other species during the study period.

The significance of the above mentioned species-specific differences in the main parameters of the CFI curve is confirmed by the results of analysis of variance of the experiment data, where the interval of values within the limits of specific indicators was 47–53%, and their formation was significantly influenced by hydrothermal conditions of vegetation in the corresponding interval of the influence share 19–29%. Given similar studies (Naidu & Long, 2004; Murata et al., 2007; Kuhlgert et al., 2016; Østrem et al., 2018; Cong et al., 2022), such a level of dependence classifies cruciferous crops as edaphic sensitive species and the chlorophyll fluorescence induction method itself as a reliable indicator of optimal or stressful agrocenosis formation of these crops. Thus, the

identified features of the formation of basic and indicative indicators of the CFI curve confirmed the possibility of their use to identify the level of stress both environmental conditions and agrotechnological factors of cultivation technology, which can be considered as systemic stress factors in the system of assessment of photosynthetic activity of plants. These conclusions are confirmed by a number of studies in the field of chlorophyll fluorescence for the analysis of stress factors of agrocenoses of various agricultural crops, in particular Arnetz (1997), Raza et al. (2017), Baker & Rosenqvist (2020), Żelazny & Lukáš (2020), Viljevac et al. (2022).

Experiment 2. Formation of CFI indicators depending on pre-sowing agro-technological construction of the oilseed radish agrocenosis

The values of the CFI curve (Table 4) give reason to affirm that the density of oilseed radish plants, sowing method and the mineral fertilizers was stress factors that affect plant growth and development, the formation of corresponding plant mass and corresponding levels of photosynthetic activity. It was determined that the value of the F_0 criterion decreases with the reduction of the area of plant nutrition.

A constant tendency to decrease F_0 within the studied options and the minimum values of this indicator for the maximum area of plant nutrition (variant 0.5 million germinable seeds ha^{-1}) was established. The indicative reaction of oilseed radish plants to the change in the density of the agrocenosis in the reaction of photosynthetic processes was confirmed.

Given the steady downward trend in F_0 within the studied variants and the minimum values of this indicator at minimum seeding rates for both sowing methods, oilseed radish should be attributed to species with a highly sensitive response to its agrocenosis density, which will be indirectly expressed in photosynthetic processes as well. The percentage reduction in F_0 in comparing the seeding rates thresholds was 24.0% for row sowing and 19.7% for wide-row sowing.

The percentage decrease in the value of F_0 for the averaged fertilizer group in the comparison of marginal technological options for row sowing was 24.0%, and for the same interval of wide-row sowing 19.7%. In fact, the studied options detailed the configuration of the area of nutrition of oilseed radish plants. With the row method of sowing, it approaches a square shape, and with wide-row sowing, it approaches a rectangular shape. That is, the change in the configuration of the power supply area affected the CFI indicators. Judging by the dynamics of oilseed radish, it was tolerant to higher levels of density in a row, provided that the inter-row distance is optimized accordingly. According to the value of F_0 on variants of 30 cm row spacing, the value of reducing the distance between plants in a row within 5% of the technologically appropriate will not significantly affect the intensity of photosynthetic reactions of the PSII photosystem of plants. At the same time, the use of mineral fertilizers had a twofold effect. Fertilization in the application rate of $N_{90}P_{90}K_{90}$ in variants with a minimum plant nutrition area (1.67×15.0 cm) ensured an increase in F_0 by an average of 17.0%, creating the prerequisites for plant miniaturization and the formation of depressed architecture (noted in the studies of Cui et al. (2003)). At the same time and also enhances competitive physiological growth plant processes, causes its idiotipic depression, signs of decreased chlorophyll content (by colour change) and acceleration of the intensity of phenological staging of the assimilating plant surface.

Table 4. Baseline and estimated indicators of the CFI curve in the oilseed radish variety 'Zhuravka' depending on technological variants of pre-sowing agro-technological construction its agrocenosis, 2015–2020 (in relative units for flowering phase BBCH 65)

Plant placement	Fertilizer	Basic indicators				Estimated indicators and indices											
		F_0	F_{pl}	F_m	F_{st}	dF_{pl}	F_v	dF_{pl}/F_v	EP	L_{wp}	Q_{ue}	RF_d	K_{ef}	QP	K_{prp}	K_{fd}	V_t
4.0 million, row	1	565	662	1,420	615	97	855	0.113	0.602	2.51	0.661	1.309	0.433	0.942	1.513	2.309	0.058
	2	581	684	1,571	637	103	990	0.104	0.630	2.70	0.587	1.466	0.405	0.943	1.704	2.466	0.057
	3	624	677	1,512	684	53	888	0.060	0.587	2.42	0.703	1.211	0.452	0.932	1.423	2.211	0.068
	4	661	697	1,478	725	36	817	0.044	0.553	2.24	0.809	1.039	0.491	0.922	1.236	2.039	0.078
3.0 million, row	1	522	612	1,509	557	90	987	0.091	0.654	2.89	0.529	1.709	0.369	0.965	1.891	2.709	0.035
	2	536	630	1,611	584	94	1,075	0.087	0.667	3.00	0.499	1.759	0.363	0.955	2.006	2.759	0.045
	3	546	632	1,644	598	86	1,098	0.078	0.668	3.01	0.497	1.749	0.364	0.953	2.011	2.749	0.047
	4	561	625	1,608	617	64	1,047	0.061	0.651	2.87	0.536	1.606	0.384	0.947	1.866	2.606	0.053
2.0 million, row	1	492	641	1,735	526	149	1,243	0.120	0.716	3.53	0.396	2.298	0.303	0.973	2.526	3.298	0.027
	2	500	662	1,791	543	162	1,291	0.125	0.721	3.58	0.387	2.298	0.303	0.967	2.582	3.298	0.033
	3	503	681	1,819	552	178	1,316	0.135	0.723	3.62	0.382	2.295	0.303	0.963	2.616	3.295	0.037
	4	514	675	1,824	567	161	1,310	0.123	0.718	3.55	0.392	2.217	0.311	0.960	2.549	3.217	0.040
1.0 million, row	1	461	655	1,824	488	194	1,363	0.142	0.747	3.96	0.338	2.738	0.268	0.980	2.957	3.738	0.020
	2	464	674	1,902	490	210	1,438	0.146	0.756	4.10	0.323	2.882	0.258	0.982	3.099	3.882	0.018
	3	463	692	1,944	484	229	1,481	0.155	0.762	4.20	0.313	3.017	0.249	0.986	3.199	4.017	0.014
	4	459	711	1,978	477	252	1,519	0.166	0.768	4.31	0.302	3.147	0.241	0.988	3.309	4.147	0.012
2.0 million, wide-row	1	505	642	1,690	576	137	1,185	0.116	0.701	3.35	0.426	1.934	0.341	0.940	2.347	2.934	0.060
	2	515	667	1,718	592	152	1,203	0.126	0.700	3.34	0.428	1.902	0.345	0.936	2.336	2.902	0.064
	3	543	672	1,704	624	129	1,161	0.111	0.681	3.14	0.468	1.731	0.366	0.930	2.138	2.731	0.070
	4	562	663	1,694	651	101	1,132	0.089	0.668	3.01	0.496	1.602	0.384	0.921	2.014	2.602	0.079
1.5 million, wide-row	1	498	671	1,808	551	173	1,310	0.132	0.725	3.63	0.380	2.281	0.305	0.960	2.631	3.281	0.040
	2	505	694	1,876	559	189	1,371	0.138	0.731	3.71	0.368	2.356	0.298	0.961	2.715	3.356	0.039
	3	509	709	1,952	561	200	1,443	0.139	0.739	3.83	0.353	2.480	0.287	0.964	2.835	3.480	0.036
	4	511	703	1,935	571	192	1,424	0.135	0.736	3.79	0.359	2.389	0.295	0.958	2.787	3.389	0.042

Table 4 (continued)

1.0	1	459	659	1,847	503	200	1,388	0.144	0.751	4.02	0.331	2.672	0.272	0.968	3.024	3.672	0.032
million,	2	457	674	1,894	492	217	1,437	0.151	0.759	4.14	0.318	2.850	0.260	0.976	3.144	3.850	0.024
wide-row	3	455	692	1,929	484	237	1,474	0.161	0.764	4.24	0.309	2.986	0.251	0.980	3.240	3.986	0.020
	4	452	703	1,987	497	251	1,535	0.164	0.773	4.40	0.294	2.998	0.250	0.971	3.396	3.998	0.029
0.5	1	432	668	1,956	481	236	1,524	0.155	0.779	4.53	0.283	3.067	0.246	0.968	3.528	4.067	0.032
million,	2	428	683	2,028	475	255	1,600	0.159	0.789	4.74	0.268	3.269	0.234	0.971	3.738	4.269	0.029
wide-row	3	425	711	2,104	465	286	1,679	0.170	0.798	4.95	0.253	3.525	0.221	0.976	3.951	4.525	0.024
	4	421	719	2,189	457	298	1,768	0.169	0.808	5.20	0.238	3.790	0.209	0.980	4.200	4.790	0.020

$LSD_{0.5}$	F_0	F_{pl}	F_m	F_{st}
$LSD_{0.5}$ factor A (year)	4.81	5.74	5.90	3.70
$LSD_{0.5}$ factor B (sowing method)	2.77	3.31	3.40	2.14
$LSD_{0.5}$ factor C (seeding rate)	3.92	4.68	4.82	3.02
LSD_{05} factor D (fertilizer)	3.92	4.68	4.82	3.02
$LSD_{0.5}$ interaction AB	6.80	8.11	8.34	5.24
$LSD_{0.5}$ interaction AC	9.61	11.47	11.79	7.41
$LSD_{0.5}$ interaction AD	9.61	11.47	11.79	7.41
$LSD_{0.5}$ interaction BC	5.55	6.62	6.81	4.28
$LSD_{0.5}$ interaction BD	5.55	6.62	6.81	4.28
$LSD_{0.5}$ interaction CD	7.85	9.37	9.63	6.05
$LSD_{0.5}$ interaction ABC	13.59	16.22	16.68	10.47
$LSD_{0.5}$ interaction ABD	13.59	16.22	16.68	10.47
$LSD_{0.5}$ interaction ACD	19.22	22.94	23.59	14.81
$LSD_{0.5}$ interaction BCD	11.10	13.25	13.62	8.55
$LSD_{0.5}$ interaction ABCD	27.19	32.44	33.36	20.95

The share of influence of experimental factors				
factors	F_0	F_{pl}	F_m	F_{st}
A	20,116	40,244	28,095	29.970
B	19,330	8,447	19,545	6,330
C	26.595	9.473	42.346	39.300
D	13.462	16.431	5.662	12.670
AB	0.020	0.009	0.076	0.023
AC	0.028	0.010	0.164	5.240
AD	0.014	0.017	0.022	0.010
BC	11,908	21.323	2.579	1.224
BD	2.613	0.240	0.038	0.732
CD	2.380	2,762	0.496	4.333
ABC	0.013	0.022	0.010	0.005
ABD	0.003	0.001	0.001	0.003
ACD	0.003	0.003	0.002	0.016
BCD	3,511	1.017	0.960	0.143
ABCD	0.004	0.001	0.004	0.001

A factor – year conditions. Fertilizer options consistently: 1 – $N_0P_0K_0$; 2 – $N_{30}P_{30}K_30$; 3 – $N_{60}P_{60}K_{60}$; 4 – $N_{90}P_{90}K_{90}$.

The analysis of the F_0 indicator for other technological options of the plant nutrition area allowed to determine the optimal rates of fertilizers. It was $N_{30}P_{30}K_{30}$ for the interval 3.0–4.0 million germinable seeds ha^{-1} and $N_{60}P_{60}K_{60}$ for the interval 1.5–2.0 million germinable seeds ha^{-1}. For the remaining technological variantss, it can be increased to $N_{60}P_{60}K_{60}$. These results are also confirmed by the values of the other two basic parameters of the CFI curve, Fpl and Fm, which demonstrated similar dynamics of changes within the studied variants.

It was established that under conditions of saturated light intensity, the maximum value of fluorescence on the induction curve was due to the dynamic balance between the processes of fluorescence, photochemistry, and thermal dissipation. It is believed that at point Fm, under conditions of maximum fluorescence, photosynthesis is at a minimum level.

This index is the most variable of all others due to adaptive changes in the structure of the pigment complex (Nesterenko et al. (2006). When there is insufficient light, both light-gathering and aerial chlorophylls increase, which is accompanied by an increase in the F_m level (Brestic & Zivcak, 2013). These are the reasons that lead to the largest range of F_m values, both when evaluating the formation of CFI curve indicators in different types of cruciferous crops (Table 3) and its value for the studied variants (Table 4).

The dynamics of formation of Fm was similar to the change of the F_0 indicator. It was established that the optimal variants of the plant nutrition area also had a higher F_m index. This is explained by the reaction of the F_{pl}–F_m section of the CFI curve to factors such as changes in plant illumination, damage to the photosystem by various types of infections and pests, chlorophyll concentration, and the level of mineral nutrition. On the basis of this, the optimal agrotechnological intervals for the nutrition area of oilseed radish plants was similar to the determination based on the evaluation of the F_0 index. Similar conclusions were made in other studies (Janušauskaite & Feiziene, 2012; Tikkanen et al., 2014; Kalaji et al., 2017 and 2017b; Tsai et al., 2019; Hou et al., 2021; Tomaškin et al., 2021; Valcke, 2021).

We should also note a certain specificity of fluorescence formation of the 'plateau' zone F_{pl}, the value of which had a more significant response to the fertilizer system than to the variants of seeding rate and seeding method. This is indicated by the values of the factor influence results in the multifactor dimensional analysis system, where the latter accounted for 8.4–9.5% and the fertilizer for 16.4%. We assume that this dependence can be explained by the nature of the F_{pl} value. The fluorescence index at the F_{pl} level is due to rapid energy saturation by reaction centres (RC) that do not transfer energy to the electron-transport chain (they do not recover the primary acceptor QA and thus there are reaction centres that do not recover the electron-transport chain). The F_{pl} index expresses the slowing down stage of the CFI curve and determines certain species-specific features of the levels of plant photosystem organization. The species specificity in this case is characterized by a rather narrow interval spectrum of F_{pl} values within the range of 610–720 relative units with predominance of even narrower interval of 630–660 relative units. Additional mineral nutrition due to the optimization of the photosystem and the increase in the concentration of chlorophyll (which was noted in the studies of Nesterenko et al. (2006) and Kalaji et al. (2017 and 2017a)) provided higher F_{pl} values.

It should be noted that the EP (F_v/F_m) index we mentioned earlier, known in the literature as the 'maximum quantum efficiency' of PSII (Kalaji et al., 2017b) is a measure sensitive to photosynthetic productivity and effective in assessing photoinhibition.

Researchers experimentally determined for other plants that this indicator heads towards 1 when the physiological state of the plant is normal (Korneev, 2002; Kalaji et al., 2017a). According to these statements, the possibility of significantly optimizing the functioning of the photosystem of oilseed radish plants in such options as 1.0 million germinable seeds ha^{-1} (row spacing 15 cm, $N_{90}P_{90}K_{90}$) and 0.5 million germinable seeds ha^{-1} (row spacing 30 cm, $N_{90}P_{90}K_{90}$) was established. For these variants, the EP indicator was 0.768 and 0.808, respectively.

The defined variants are characterized by the highest plant viability index (RF_d), high level of leaf water potential (L_{wp}), which essentially indicates the physiological activity of leaves and the level of their watering (Lei et al., 2006; Evans, 2009). Other positive features of these variants are the reduced photochemical quenching (Q_{ue}) and the significantly higher photosynthetic primary reaction efficiency (K_{prp}) and the lowest endogenous stress factor level (K_{ef}). When comparing the variants 4.0 million pcs. ha^{-1} of germinable seeds and 0.5 million pcs. ha^{-1} of germinable seeds, we should note a 23.8% decrease in the intensity of photochemical reactions. According to Valcke (2021) this pattern of ratio makes the variant of oilseed radish cultivation by row seeding with the rate of 4.0 million pcs. ha^{-1} of germinable seeds to be clearly stressful with formation of plants with reduced vitality morphological and physiological features and ultimately forms a significantly lower biomass and seed productivity of the cenosis.

The conclusions made above and the results of the evaluation of criterion F_{st} are confirmed. It is worth noting that the degree of decrease in chlorophyll fluorescence from maximum (F_m) to steady-state (F_{st}) is often used as an integral indicator of the activity of the photosynthetic apparatus of plants. It was noted (Nesterenko et al., 2006; Logan et al., 2014; Jonathan, 2017) that F_{st} index the amount of chlorophyll not involved in energy transfer to PSII reaction centres. An increase in this index indicates an inhibition of the outflow of reduced photoproducts from reaction centres as a result of unfavourable environmental factors. It is noted, that the value of this index can serve to diagnose the intensity of the stress factor by estimating the time of its achievement on the CFI curve, the ratio of its value between the initial chlorophyll fluorescence induction (F_0) and its maximum value, and by comparing the difference between the value of F_0 and F_{st} (Roháček, 2002; Nesterenko et al., 2012; Schreiber & Klughammer, 2013; Murchie et al., 2018). Moreover, Flexas et al. (2002) recommend the use of steady-state fluorescence to indicate the water status of plants by the ratio of F_{st} and F_0. For oilseed radish was established that the value of the steady-state fluorescence Fst is higher than the value of its initial level F_0. This difference amounted to 27–71 conventional fluorescence units.

It is important to note, that chloroplasts of oilseed radish leaves in the variants of higher area of plant nutrition with a maximal fertilization rate are characterized by a considerable drop of chlorophyll fluorescence from F_m to stationary level F_{st}, that is a sign of intensive course of dark photochemical reactions, which is an evidence of optimization of vitamin tactics and physiological photochemical processes of plants. Certain aspects of this were confirmed by research Sepúlveda & Johnstone (2019), Schuback et al. (2021).

It is installed that the F_{st} value for variants with maximum density of oilseed radish plants had significantly higher values than in the variants with minimum density. When applied to the F_{st} index, the optimality of the technological variant can be assessed by comparing the F_0 and F_{st} indexes. Closeness of their values against the background of considerably according to F_m index criterion results in decrease of the indicator of

endogenous (stress) factors K_{ef}, the value of which characterizes the total intensity of stress on edaphic conditions (according to Schreiber & Klughammer, 2013; Ruban et al., 2016) and increases the value of photochemical quenching of fluorescence QP (according to Schreiber et al., 1995; Maxwell & Johnson, 2000; Korneev, 2002; Larouk et al., 2021)). Thus, in comparing the variants 4.0 and 0.5 million pcs. ha^{-1} of germinable seeds the value of K_{ef} was 47.6% lower for the lower limit variant of nutrition area. The level of QP was higher on the average by 3.8% on the background the reduction of the rate of relative variable fluorescence (V_t) by 57.7% and increasing of the rate of photosynthetic primary reactions (K_{prp}) by 2.8 times.

Specific information about the physiological state of plants within the studied experimental variants was obtained by analyzing the ratio $dF_{pl}\ F_v^{-1}$. However, under these excitation light conditions, this ratio can characterise the infectivity of the plants with viruses (according to Korneev, 2002; Bonfig et al., 2006; Christen et al., 2007; Romanov et al., 2010; Burling et al., 2011; Amri et al., 2021). In particular, in research Kirik et al. (2011) an excess of dF_{pl}/F_v over 0.4 at excitation light intensities that do not saturate the pigment matrix in energy indicates a high probability of plant viral infection.

In our studies, this coefficient was in the range 0.044–0.170 within the variants, which may indicate that the plants are not infected with viral infection. Still, the tendency for its value to increase with decreasing seeding rate and, consequently, the density of the plants, indicates an increase in the potential for plant infections in oilseed radish by optimizing growth processes, an intensive increase in vegetative mass, and as was shown earlier before the increase of leaf watering by the water potential indicator L_{wp}.

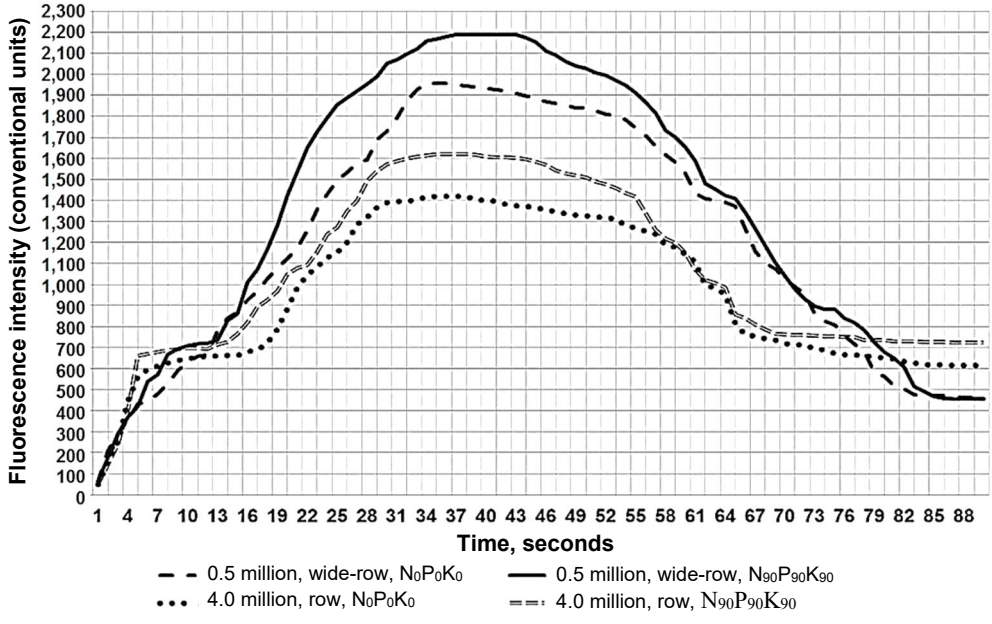

Figure 5. Induction changes of CFI curves in oilseed radish variety 'Zhuravka' under different variants of research, average data 2015–2020.

Visualization of the peculiarities of the formation of the parameters of the CFI curve (Fig. 5) clearly confirmed the described results. The overall stressfulness of the variant

with 4.0 million pcs. ha^{-1} of germinable seeds according to the main accounting basic parameters has been confirmed. This interval as stressful can also be identified by the characteristic part of the CFI curve (62–65 seconds of registration) of beveled plateau-like character, which at a lower plant nutrition area had a shorter fixation period and less pronounced character with a smoother transition to steady fluorescence (F_{st}). This is confirmed by the results of the visual assessment of the CFI curves for the different plant species carried out in the studies by Lootens et al. (2004), Lichtenthaler et al. (2005), Baležentienė & Šiuliauskienė (2007), Brestic & Zivcak (2013), Murchie & Lawson (2013), Kalaji et al. (2017b).

Our conclusions are also supported by the results of the summary cluster analysis of the baseline indicators of the CFI curve (Fig. 6). By value of Euclidean distance, variants with seeding rates of 4.0 and 3.0 million pcs. ha^{-1} of germinable seeds in row sowing have essential criterial distance in values of induction indices in relation to variants with seeding rates in the interval of 0.5–1.0 million pcs. ha^{-1} of germinable seeds. As for seeding methods, the nature of the Euclidean distance indicates that the intensity of the decrease in the values in the cluster system for string sowing covers agrotechnological variants from 2.0 million pcs. ha^{-1} of germinable seeds without fertilizer to 3.0–4.0 million pcs. ha^{-1} of similar seeds for all variants. application of fertilizer. For wide-row sowing, this interval has a smaller technological range and includes variants from 1.5 million pcs. ha^{-1} of germinable seeds without fertilizer to 2.0 million pcs. ha^{-1} of germinable seeds against all fertilizer options.

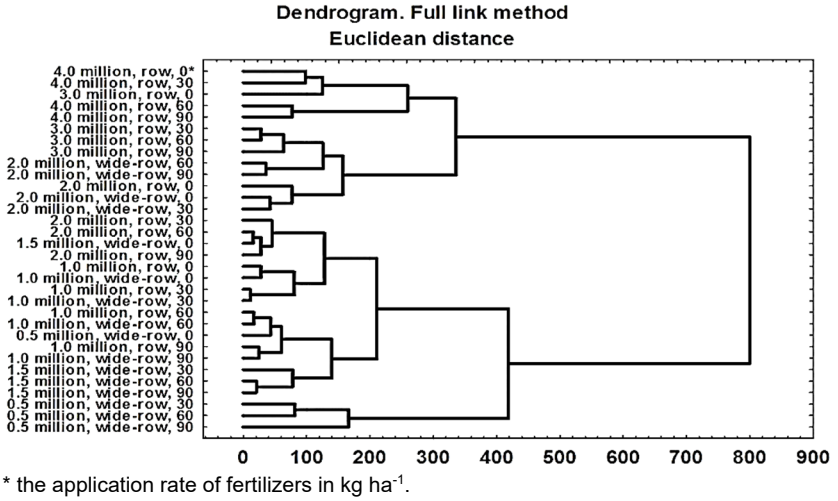

Figure 6. Dendrogram of cluster analysis (full link method) for baseline indicators of CFI curve in the context of the studied technological variants, average data 2015–2020.

Based on this, it was concluded that from the position of providing the optimization of photosynthetic apparatus activity of oilseed radish plants the configuration of plant nutrition area is essential for oilseed radish, and the change of row spacing allows to shift the expediency of applied seeding rate to higher level of predicted calculation of plant productivity increase its biological level. That is to say with reference of Driever et al. (2014) the combination of appropriate levels of plant photoassimilation with predicted productivity of 1 m^2 of accounting area was achieved.

The results of summary clustering of data allow and confirm the stress of application of high rates of fertilizers with an increase in seeding rate over 2.0 million pcs. ha^{-1} of germinable seeds for row sowing of oilseed radish and over 1.5 million pcs. ha^{-1} of germinable seeds for wide-row sowing variant. This indicates the closeness of Euclidean distances for variants with the absence of fertilizer and variants with a fertilization rate of $N_{90}P_{90}K_{90}$.

This is confirmed by the closeness of the Euclidean distances for variants with a fertilizer rate of 0 and 90 kg ha^{-1}. With an increase in the area of plant nutrition, paired systems of combinations of Euclidean distances were noted in the variants of technological pairs of 60–90 kg ha^{-1} for close technological groups in terms of the area of plant nutrition.

More detailed and deep analysis of the features of CFI curve indication is performed by their correlation in a single system, which, according to Larouk et al. (2021) allows to determine the combinatorics of its influence in the physiological process of photoassimilation and plant photosystem functioning. Based on the values, the strongest correlations are found for the maximum fluorescence (F_m) with high marginal correlation values, either directly or inversely related to other indicators in a pairwise correlation (Table 5). Accordingly, the least significant correlation among the correlation pairs of the comparison is found for the 'plateau' zone fluorescence indicator (F_{pl}). In our opinion, this can be explained by the nature of the role of these indicators in the dynamic processes and energetics of the CFI curve formation. The Fm value is the main indicator of the fluorescence process, which determines the overall intensity of the process and the psolidating nature of its attenuation rates. The range of correlation coefficients is intrinsic to the system of such analyses, as observed in both the earlier (Korneev, 2002), and more recent (Bussotti et al., 2020; Larouk et al., 2021; Rao et al., 2021) publications. It is noted that the value of the correlation can change both in magnitude and direction.

Table 5. Range of the correlation coefficients of the CFI curve (range of values during 2015–2020)

	F_{pl}	F_m	F_{st}	F_v	EP	L_{wp}	Q_{ue}	ISP
F_0	0.634– 0.732***	-0.468**– -0.844***	0.394*– 0.768***	-0.387*– -0.792***	-0.454**– -0.846***	-0.602**– -0.945***	0.396*– 0.946***	-0.381*– -0.601**
F_{pl}		0.342*– 0.487**	-0.076ns– -0.275*	0.243*– 0.334*	0.090 ns– 0.262*	0.094 ns – 0.264*	0.053 ns – -0.264*	0.426**– 0.569**
F_m			-0.643**– -0.807***	0.762***– 0.992***	0.731***– 0.963***	0.728***– 0.964***	-0.730***– -0.964***	0.628**– 0.839***
F_{st}				-0.642**– -0.840***	-0.680**– -0.910***	-0.681**– -0.910***	0.680**– 0.911***	-0.505**– -0.641**
F_v					0.739***– 0.986***	0.727***– 0.981***	-0.718***– -0.977***	0.678**– 0.818***
EP						0.763***– 0.987***	-0.732***– -0.985***	0.451**– 0.773***
L_{wp}							-0.755***– -0.989***	0.449***– 0.779***
Q_{ue}								-0.459**– -0.775***

Legend: ISP – Individual Seed Productivity (g $plant^{-1}$); ns not significant at 5%; *, **, *** Significant at 5%, 1%, 0.1% level probability, respectively.

This process is primarily influenced by stress factors such as drought, high or low temperatures, plant diseases or viral infection. In our case, we observed only a significant decrease in the indicator across a range of dependencies, often in the range of two or threefold decrease, as Table 5 clearly shows. It should be noted that the tightness of the relationship increased as the stress of the year increased and, conversely, tended to decrease as the parameters optimised. However, cases of directional changes in dependence were rare. According to the findings of Bussotti et al. (2020), this indicates that the baseline indicators of the CFI curve for oilseed radish can be used in a system for assessing the adaptive strategy in terms of its vitality tactics.

An indicator of seed productivity of plants was introduced into the system of correlations, as a result criterion of the optimality of the area of plant nutrition.

Analysis of the seed yield of oilseed radish plants within the studied agrotechnological variants (Fig. 7) showed significant differences between them in the value of the existing indicator of the biological level of individual seed productivity over a multi-year evaluation period.

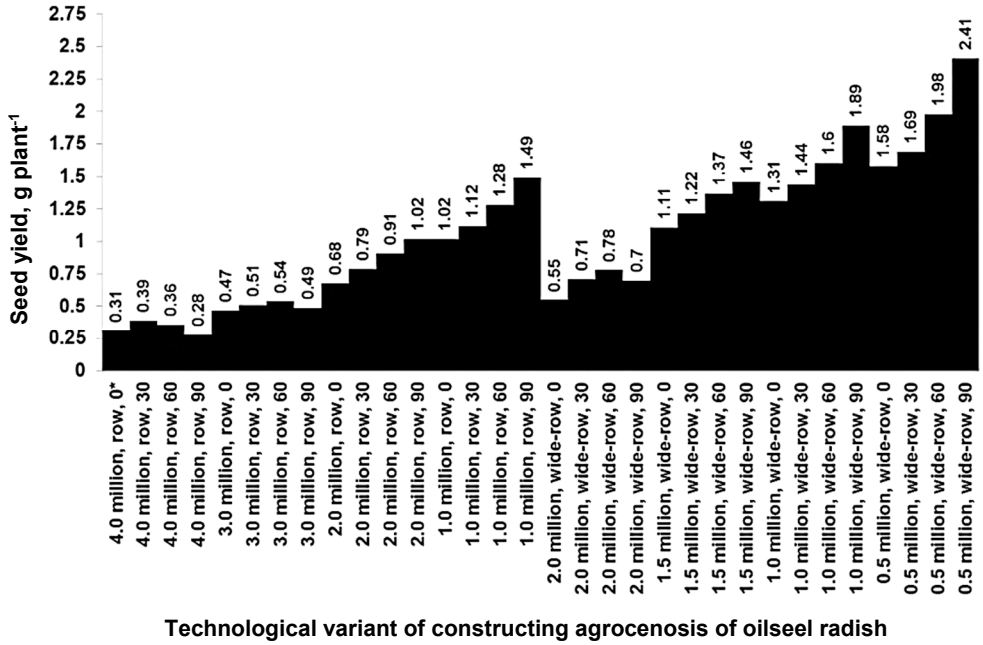

Figure 7. Individual seed productivity of oilseed radish plants (biological level) of 'Zhuravka' variety in various variants of experiment 2, average data 2015–2020.

(For factors A – year, B – sowing method, C – seeding rate, D – fertilizer: LSD_{05}: A – 0.08, B – 0.05, C – 0.06, D – 0.06, AB – 0.11, AC – 0.16, AD – 0.16, BC – 0.09, BD – 0.09, CD – 0.13, ABC – 0.22, ABD – 0.22, ACD – 0.32, BCD – 0.18, ABCD – 0.45. Fraction of the resultant effect of experience factors on the resultant trait (%): A 21.75; B 14.10; C 34.73; D 12.25; AB 1.89; AC 2.31; AD 1.00; BC 4.96; BD 0.75; CD 4.17; ABC 0.84; ABD 0.14; ACD 0.47; BCD 0.40; ABCD 0.25).

Noted the steady growth of seed yield from a plant for the growth of the nutrition of plant. The overall average growth in the comparison of variants of row-crop and wide-row sowing was 1.82. This means that a change in the configuration of the feeding area

has a positive effect on the formation of the reproductive effort of plants and its assimilative activity. Fertilizers in general had a positive effect on the level of seed yield from the plant, providing an average increase of 9.6% to the control. The effect of fertilizer application was significantly different. Within the variants of row sowing, increases from growth of fertilizers rate to 60 kg ha^{-1} (nitrogen, phosphorus and potassium) at the level of 5–11% were considered for variants 3.0–4.0 million pcs. ha^{-1} of germinable seeds. An increase in the fertilizers rate up to 90 kg ha^{-1} (nitrogen, phosphorus and potassium) for these variants did not form the subsequent growth, but on the contrary had the opposite effect in comparison with the fertilizers rate of 60 kg ha^{-1} (nitrogen, phosphorus and potassium). In general, we noted a pattern of increase in growth from the use of fertilizer in comparison with the previous version of the fertilizer with an increasing pattern for both increasing the width of row spacing and reducing the seeding rate. Thus, the average growth rate of fertilizer for row sowing was 7.1% for the period of research, and for wide-row sowing - 11.9%. The minimum increase of 4.0–5.0% was recorded in variants with seeding rate of 3.0–4.0 million pcs. ha^{-1} of germinable seeds, and the maximum increase of 16.4–21.7% in variants with 1.0 million pcs. ha^{-1} of germinable seeds for row sowing and 0.5 million pcs. ha^{-1} of germinable seeds for wide-row sowing. At the same time, the performance of individual seed production was significantly influenced by the weather conditions of the growing season, with the factor share of the impact of agri-environmental factors of the year in the system of studied variants was 21.75%. Based on the climatic resources of the research region the yield of oilseed radish seeds of the studied genotypes varies from 1.1 to 2.5 t ha^{-1} and corresponds to the potential of the studied varieties of oilseed radish (Tsytsiura, 2019, 2020), and the yield is the integration of standing density and individual productivity of one plant, the most appropriate variant should be considered in the interval of 1.0–2.0 million pcs. ha^{-1} of germinable seeds at row sowing with the fertilizers rate 30–60 kg ha^{-1} (nitrogen, phosphorus and potassium) of fertilization and 1.5 million pcs. ha^{-1} of germinable seeds at row sowing with the fertilizers rate 60–90 kg ha^{-1} (nitrogen, phosphorus and potassium).

Although these variants do not exhibit the effective-optimal level of the CFI curve for a number of indicators (emphasis added above), the level achieved in the experiment, combined with factors of the appropriate reproductive architectonics of the plants, is sufficient to obtain the maximum yield in the system of variants of the experiment. This is also confirmed by the results of the correlation analysis (Table 5). According to the obtained values of the correlation coefficients, the basic indicators of the CFI curve can be used in predicting the yield of oilseed radish seeds. This possibility is confirmed for a number of cruciferous crops in studies Guo et al. (2005), Jamil & Rha (2013), Athar et al. (2015), Kalaji et al. (2018), Bukhat et al. (2020), Ayyaz et al. (2021), De Canniére & Jonard (2021).

The magnitude of the correlation coefficients associated with the ISP indicator proved a significant negative correlation between the yield seeds of oilseed radish and such indicators of the CFI curve as F_0, F_{st}. The direct significant correlation was determined for F_{pl}, F_m, F_v, EP, L_{wp} and Q_{ue}. Given the variation in closeness of relationship and the recommendations of Arkes (2019), the most reliable criteria for predicting individual levels of seed production of oilseed radish plants will be F_m, F_v and their ratios. Similar results, given the biological and physiological specificity of cruciferous plants, were

reported in studies with rapeseed and white mustard by Jamil & Rha (2013) and Kalaji et al. (2018). However, the evaluation period of these authors was shorter or compared to typical and stressed years.

The role of weather conditions in the formation of indicators of the CFI curve

The aspect of significant influence on chlorophyll fluorescence hydrothermal regime of the year is not new. A number of recent generalized publications (Brestic & Zivcak, 2013; Abid et al., 2016; Kalaji et al., 2017b; Jedmowski et al., 2015; Hamann, 2021; Larouk et al., 2021; Moore et al., 2021; Lin et al., 2022; Wang et al., 2022) emphasize both the influence on the magnitude and expression of the basic criteria of the CFI curve of temperature and moisture regime, and their systemic impact on the overall nature of photosynthetic activity of the assimilative surface of plants. These conclusions was supported by the results of the assessment of baseline and estimated CFI curve indicators for the most stressful conditions in 2015 (Table 2, Fig. 1) presented in Table 6.

Changes were assessed against a total six-year study period in which three years was stressful (aridity, high average daily temperatures) in terms of HTC (2015, 2016, 2017) and three with near-optimal temperature regimes against excessive moisture (2018–2020). (Table 2). It allowed to use the six-year test cycle as a statistically valid comparison to the most stressful year according to McDonald (2014). The obtained results indicate an overall decrease in the aggregate system of agro-technological options as a percentage comparison with the average annual cycle of counts for the period 2015–2020: F_{pl} by 1.3%, F_m by 11.8%, EP by 8.7%, L_{wp} by 15.9%, RF_d by 25.3%, K_{prp} by 21.9%, K_{fd} by 17.7%. At the same time, there was an increase in the following indicators: F_0 by 5.1%, F_{st} by 7.3%, Q_{ue} by 40.4%, K_{ef} by 24.0%, V_t by 71.3%. Thus, for oilseed radish in general, with a significant decrease in moisture supply against the background of an intensive increase in average daily temperatures is characterized by a general decrease in the amplitude of the curve CFI against the background of increasing fluorescence 'plateau' zone (F_{pl}) and the value of steady-state fluorescence (F_{st}).

This results in an overall increase in overall plant stress and a decrease in plant vitality according to the given reduction dynamics of the criteria L_{wp}, RF_d, K_{prp} and K_{fd}. Against this background the intensity of the relative variable fluorescence at time t (V_t) increases significantly, indicating an increase in the reaction rate in the F_m–F_{st} part of the curve with an earlier shift of 3–4 seconds in the F_{st}-achieving point. This is clearly confirmed by the data in Fig. 8 within the limits of the technological variants studied in 2015.

In addition, for the stressful 2015 of the lines of the CFI curve had a pronounced microrelief oscillating character with a weakly pronounced 'plateau zone' in the range of 62–65 seconds, especially in the case of maximum density of agrocenosis of oilseed radish. At the same time, the maximum reduction of indicators by the specified general tendency was observed for seeding rates in the range of 3.0–4.0 million germinable seeds ha^{-1} at row sowing with maximum effect in variants of application fertilizing rate of $N_{30–60}P_{30–60}K_{30–60}$ and rates in the range of 1.5–2.0 million germinable seeds ha^{-1} with fertilizing rate of $N_{90}P_{90}K_{90}$ at wide-row sowing. However, there was a significant difference in plant stress response between row sowing and wide-row sowing with an averaging factor of 1.117 in the wide-row/row sowing system.

Table 6. Baseline and estimated indexes of the CFI curve in the oil radish variety 'Zhuravka' depending on technological variants of pre-sowing design of its agrocenosis, 2015 (in relative units of the fluorescence on the phase of flowering BBCH 65)

Plant placement	Fertilizer	Basic indicators				Estimated indicators and indices											
		F_0	F_{pl}	F_m	F_{st}	dF_{pl}	F_v	dF_{pl}/F_v	EP	L_{wp}	Q_{ue}	RF_d	K_{ef}	QP	K_{prp}	K_{fd}	V_t
4.0 million, row	1	579	655	1,160	629	76	581	0.131	0.501	2.00	0.997	0.844	0.542	0.914	1.003	1.844	0.086
	2	590	671	1,284	654	81	694	0.117	0.540	2.18	0.850	0.963	0.509	0.908	1.176	1.963	0.092
	3	638	689	1,127	707	51	489	0.104	0.434	1.77	1.305	0.594	0.627	0.859	0.766	1.594	0.141
	4	687	711	1,057	755	24	370	0.065	0.350	1.54	1.857	0.400	0.714	0.816	0.539	1.400	0.184
3.0 million, row	1	533	603	1,348	594	70	815	0.086	0.605	2.53	0.654	1.269	0.441	0.925	1.529	2.269	0.075
	2	548	621	1,409	625	73	861	0.085	0.611	2.57	0.636	1.254	0.444	0.911	1.571	2.254	0.089
	3	568	628	1,307	642	60	739	0.081	0.565	2.30	0.769	1.036	0.491	0.900	1.301	2.036	0.100
	4	590	618	1,265	665	28	675	0.041	0.534	2.14	0.874	0.902	0.526	0.889	1.144	1.902	0.111
2.0 million, row	1	511	633	1,568	556	122	1,057	0.115	0.674	3.07	0.483	1.820	0.355	0.957	2.068	2.820	0.043
	2	521	648	1,602	578	127	1,081	0.117	0.675	3.07	0.482	1.772	0.361	0.947	2.075	2.772	0.053
	3	535	668	1,529	596	133	994	0.134	0.650	2.86	0.538	1.565	0.390	0.939	1.858	2.565	0.061
	4	551	661	1,495	618	110	944	0.117	0.631	2.71	0.584	1.419	0.413	0.929	1.713	2.419	0.071
1.0 million, row	1	478	645	1,633	517	167	1,155	0.145	0.707	3.42	0.414	2.159	0.317	0.966	2.416	3.159	0.034
	2	486	661	1,744	524	175	1,258	0.139	0.721	3.59	0.386	2.328	0.300	0.970	2.588	3.328	0.030
	3	492	677	1,655	526	185	1,163	0.159	0.703	3.36	0.423	2.146	0.318	0.971	2.364	3.146	0.029
	4	501	691	1,639	539	190	1,138	0.167	0.694	3.27	0.440	2.041	0.329	0.967	2.271	3.041	0.033
2.0 million, wide-row	1	527	636	1,504	609	109	977	0.112	0.650	2.85	0.539	1.470	0.405	0.916	1.854	2.470	0.084
	2	535	665	1,588	631	130	1,053	0.123	0.663	2.97	0.508	1.517	0.397	0.909	1.968	2.517	0.091
	3	541	668	1,516	672	127	975	0.130	0.643	2.80	0.555	1.256	0.443	0.866	1.802	2.256	0.134
	4	617	659	1,461	708	42	844	0.050	0.578	2.37	0.731	1.064	0.485	0.892	1.368	2.064	0.108
1.5 million, wide-row	1	518	664	1,714	579	146	1,196	0.122	0.698	3.31	0.433	1.960	0.338	0.949	2.309	2.960	0.051
	2	529	687	1,776	594	158	1,247	0.127	0.702	3.36	0.424	1.990	0.334	0.948	2.357	2.990	0.052
	3	544	699	1,763	615	155	1,219	0.127	0.691	3.24	0.446	1.867	0.349	0.942	2.241	2.867	0.058
	4	569	690	1,669	636	121	1,100	0.110	0.659	2.93	0.517	1.624	0.381	0.939	1.933	2.624	0.061
1.0 million, wide-row	1	474	652	1,750	531	178	1,276	0.139	0.729	3.69	0.371	2.296	0.303	0.955	2.692	3.296	0.045
	2	481	663	1,811	539	182	1,330	0.137	0.734	3.77	0.362	2.360	0.298	0.956	2.765	3.360	0.044
	3	491	678	1,795	552	187	1,304	0.143	0.726	3.66	0.377	2.252	0.308	0.953	2.656	3.252	0.047
	4	509	683	1,728	570	174	1,219	0.143	0.705	3.39	0.418	2.032	0.330	0.950	2.395	3.032	0.050

Table 6 (continued)

0.5 million, wide-row	1	443	660	1,898	498	217	1,455	0.149	0.767	4.28	0.304	2.811	0.262	0.962	3.284	3.811	0.038
	2	448	674	1,962	500	226	1,514	0.149	0.772	4.38	0.296	2.924	0.255	0.966	3.379	3.924	0.034
	3	454	699	1,955	502	245	1,501	0.163	0.768	4.31	0.302	2.894	0.257	0.968	3.306	3.894	0.032
	4	456	704	1,971	509	248	1,515	0.164	0.769	4.32	0.301	2.872	0.258	0.965	3.322	3.872	0.035

$LSD_{0.5}$	F_0	F_{pl}	F_m	F_{st}
$LSD_{0.5}$ factor A (sowing method)	3.24	4.36	9.61	6.58
$LSD_{0.5}$ factor B (seeding rate)	4.58	6.16	13.60	9.30
$LSD_{0.5}$ factor C (fertilizer)	4.58	6.16	13.60	9.30
$LSD_{0.5}$ interaction AB	6.48	8.71	19.23	13.16
$LSD_{0.5}$ interaction AC	6.48	8.71	19.23	13.16
$LSD_{0.5}$ interaction BC	9.17	12.32	27.19	18.61
$LSD_{0.5}$ interaction ABC	12.97	17.42	38.46	26.31

The share of influence of experimental factors				
factors	F_0	F_{pl}	F_m	F_{st}
A	14.38	13.26	42.63	5.19
B	64.97	13.23	51.25	77.98
C	12.71	27.63	2.78	12.01
AB	2.46	39.92	2.03	0.20
AC	0.31	0.36	0.49	0.27
BC	4.77	2.78	0.70	4.27
ABC	0.40	2.81	0.12	0.09

Fertilizer options consistently: 1 – $N_0P_0K_0$; 2 – $N_{30}P_{30}K_{30}$; 3 – $N_{60}P_{60}K_{60}$; 4 – $N_{90}P_{90}K_{90}$.

The obtained data are positively correlated with a number of recent publications in this field of research such as Guidi et al. (2019), Baldocchi et al. (2020), Hamann (2021), Larouk et al. (2021), Ashrostaghi et al. (2022), Guo et al. (2022).

With similar tendencies in the basic and derived indicators of the CFI curve for oilseed radish under stress (water deficit and high average daily temperatures), certain peculiarities was we also established. The following features of the formation of the CFI curve in the conditions of the stress effect of the hydrothermal regime on the vegetation of oilseed radish were determined, in particular fixation of the parameter F_{pl} on the dynamic section of the CFI curve (no classical 'plateau' for the increase of environmental stressors), the long fixation period of the same F_m values, which creates a plateau effect in the fixation area of maximum fluorescence, the long fixation period and equal values of the stationary fluorescence (F_{st}).

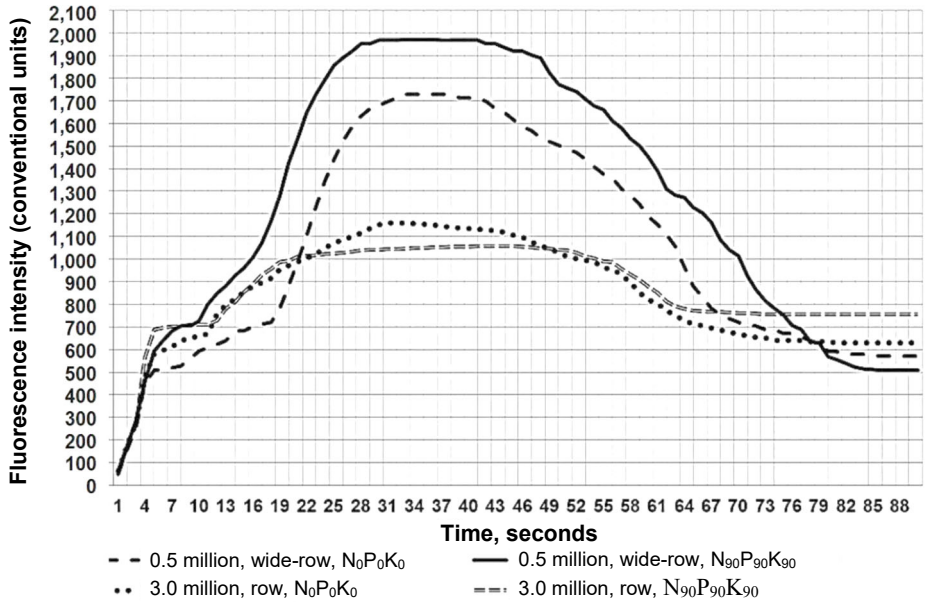

Figure 8. Induction changes of CFI curves in oilseed radish variety 'Zhuravka' under different variants for conditions of the most stressful hydrothermal regime, 2015.

Given the defined approaches for assessing plant stress responses in the general kinetics of the CFI curve according to Thach et al. (2007) and Brestic & Zivcak (2013) and Stirbet et al. (2018) oilseed radish were classified as a sensitive plant for both moisture and temperature stress parameters. This is confirmed by the simultaneous increase in F_0 and F_{st} with a disproportionate decrease in F_m against the background of the combined stress index of the hydrothermal coefficient (HTC) used in the analysis.

Interpretation of statistical evaluation of CFI curve indicators

In addition to the classical statistical data processing (ANOVA analysis), the Tukey HSD Test in R statistic was applied to the data averaged in repetitions over the period 2015–2020. Table 7 presents the results of the conducted statistical evaluation, which, in comparing successive pairs of variants, is typologically similar to the criterion '$LSD_{0.5}$

interaction BCD' (the resulting indicator of the interaction of factors in the general scheme ANOVA analysis (Table 1)).

Table 7. Tukey HSD Test results for baseline CFI curve, 2015–2020

	Df	Sum Sq	Mean Sq	F value	Pr(> F)
	F_0 index				
RE	31	154,038	4,969	11.82	< 2e-16***
Residuals	96	40,342	420		
	F_{pl} index				
RE	31	150,021	4,839	11.92	< 2e-16***
Residuals	96	38,963	406		
	F_m index				
RE	31	4,406,222	142,136	1,145	< 2e-16***
Residuals	96	11,914	124		
	F_{st} index				
RE	31	573,166	18,489	233.5	< 2e-16 ***
Residuals	96	7,602	79		

Signifscant codes: '***' 0.001; '**' 0.01; '*' 0.05; '.' 0.1; ' ' 1.

On the basis of the Tukey HSD Test, a significance matrix was constructed comparing pairs of possible combinations of research factors (Fig. 9). The specified matrix made it possible to place the basic indicators of the CFI curve of oilseed radish in relation to the reliable response of its values to the investigated agrotechnological factors in such a dynamic growth row F_0 (302 non-significant pairs of comparisons in the general scheme of factor combinations) < F_{pl} (297 non-significant pairs) < F_{st} (93 non-significant pairs) < F_m (25 non-significant pairs). The presented series corresponded to the level of physiological sensitivity of the CFI curve indicators to changes in the area of plant nutrition and its configuration under different rates of fertilizers. On the other hand, this nature of its formation in view of the statement regarding the variation of physiologically constant plant traits ensured the increasing nature of the variation of the CFI curve indexes at each point of its fixation with extrema in the sections of the curve F_0–F_{pl} and F_m–F_{st}. These statistical results, taking into account the significance of the differences between the marginal technological variants of the general experimental system for the F_0 and F_{pl} indicators, as well as the increase in the significance of the difference for technologically close variants for the F_m and F_{st} indexes, proved the possibility of using the chlorophyll fluorescence induction method for selecting the optimal variants for the nutrition area and the corresponding fertilization of oilseed radish plants.

Cstatistically confirms the conclusions made and the value of the $LSD_{0.5}$ criterion of the interaction of BCD factors according to the classical scheme of the ANOVA test (Tables 4, 6). The significance of the dimension of this criterion corresponded to the significance of the difference between pairs of comparisons for the Tukey HSD test. However, the clarity of the Tukey test is beyond doubt.

No	Ncv	1	2	3	4	5	6	7	8	9	10	11	12	13	14	15	16
1	$B_1C_1D_1$	–	c,d	c,d	c,d	c,d	a,b,c,d	a,b,c	a,b,c	a,b,c,d	a,b,c,d	a,b,c,d	a,b,c,d	a,b,c,d	a,b,c,d	a,b,c,d	a,b,c,d
2	$B_1C_1D_2$	c,d	–	c,d	c,d	c,d	a,b	a,b	a,c	a,b,c,d	a,b,c,d	a,b,c,d	a,b,c,d	a,b,c,d	a,b, c,d	a,b, c,d	a,b,c,d
3	$B_1C_1D_3$	a,b,c,d	a,b,c,d	–	c,d	d	c,d	c,d	c,d	a,b,c,d	a,b,c,d	a,b,c,d	a,b,c,d	c,d	a,b,c,d	a,b,c,d	a,b,c,d
4	$B_1C_1D_4$	a,b,c,d	a,b,c,d	c,d	–	a,b,c,d	c,d	c,d	a,c,d	a,c,d	a,c,d	a,b,c,d	a,c,d	c,d	a,c,d	a,b,c,d	a,b,c,d
5	$B_2C_1D_1$	c,d	c,d	c,d	c,d	–	c,d	c,d	c,d	c,d	a,b,c	a,b,c	a,b,c	a,b,c,d	a,b,c,d	a,b,c,d	a,b,c,d
6	$B_2C_1D_2$	c,d	c,d	c,d	c,d	c,d	–	c,d	c,d	c,d	a,b,c,d	a,b,c,d	a,b,c	c,d	a,b,c,d	a,b,c,d	a,b,c,d
7	$B_2C_1D_3$	c,d	c,d	c,d	c,d	c,d	c	–	c,d	c,d	a,b,c,d	a,b,c,d	a,b,c,d	c,d	a,b,c,d	a,b,c,d	a,b,c,d
8	$B_2C_1D_4$	c,d	c,d	c,d	c,d	c,d	d	c	–	c,d	a,b	a,b,c	a,b	c,d	a	a,b	a,b
9	$B_3C_1D_1$	c,d	c,d	c,d	c,d	c,d	c,d	c,d	c,d	–	c,d	c,d	c,d	d	a,b	a,b	a,b
10	$B_3C_1D_2$	c,d	c,d	c,d	c,d	c,d	c,d	c,d	c,d	c	–	c,d	c,d	d	c,d	c,d	a
11	$B_3C_1D_3$	c,d	c,d	c,d	c,d	c,d	c,d	c,d	c,d	a,b	c	–	c,d	a,b,d	c,d	c,d	c,d
12	$B_3C_1D_4$	c,d	c,d	c,d	c,d	c,d	c,d	c,d	c,d	a,b	c,d	d	–	a,d	c,d	c,d	c,d
13	$B_4C_1D_1$	c,d	c,d	c,d	c,d	c,d	c,d	c,d	c,d	c,d	c,d	c,d	c,d	–	c,d	c,d	c,d
14	$B_4C_1D_2$	c,d	c,d	c,d	c,d	c,d	c,d	c,d	c,d	c,d	c,d	c,d	c,d	c	–	c,d	c,d
15	$B_4C_1D_3$	c,d	c,d	c,d	c,d	c,d	c,d	c,d	c,d	c,d	c,d	c,d	c,d	a,b,c	c	–	c,d
16	$B_4C_1D_4$	c,d	c,d	c,d	c,d	c,d	c,d	c,d	c,d	c,d	c,d	c,d	c,d	a,b,c	c	c	–
17	$B_1C_2D_1$	c,d	c,d	c,d	c,d	c,d	c,d	c,d	c,d	c,d	c,d	c,d	c	c,d	c,d	a,b,c,d	a,b,c,d
18	$B_1C_2D_2$	c,d	c,d	c,d	c,d	c,d	c,d	c,d	c,d	d	c,d	c,d	c,d	c,d	c,d	c,d	a,c,d
19	$B_1C_2D_3$	c,d	c,d	c,d	c,d	c,d	c,d	c,d	c,d	c,d	c,d	c,d	c,d	c,d	c,d	c,d	a,c,d
20	$B_1C_2D_4$	c,d	c,d	c,d	c,d	c,d	c,d	c,d	c,d	c,d	c,d	c,d	c,d	c,d	c,d	a,c,d	a,c,d
21	$B_2C_2D_1$	c,d	c,d	c,d	c,d	c,d	c,d	c,d	c,d	c,d	c,d	c,d	c,d	c,d	c,d	c,d	c,d
22	$B_2C_2D_2$	c,d	c,d	c,d	c,d	c,d	c,d	c,d	c,d	c,d	c,d	c,d	c,d	c,d	c,d	c,d	c,d
23	$B_2C_2D_3$	c,d	c,d	c,d	c,d	c,d	c,d	c,d	c,d	c,d	c,d	c,d	c,d	c,d	c,d	c,d	c,d
24	$B_2C_2D_4$	c,d	c,d	c,d	c,d	c,d	c,d	c,d	c,d	c,d	c,d	c,d	c,d	c,d	c,d	c,d	c,d
25	$B_3C_2D_1$	c,d	c,d	c,d	c,d	c,d	c,d	c,d	c,d	c,d	c,d	c,d	c,d	c	c	c	c,d
26	$B_3C_2D_2$	c,d	c,d	c,d	c,d	c,d	c,d	c,d	c,d	c,d	c,d	c,d	c,d	c,d	c,d	c	c
27	$B_3C_2D_3$	c,d	c,d	c,d	c,d	c,d	c,d	c,d	c,d	c,d	c,d	c,d	c,d	a,b,c	c	c,d	c
28	$B_3C_2D_4$	c,d	c,d	c,d	c,d	c,d	c,d	c,d	c,d	c,d	c,d	c,d	c,d	a,b,c	c	c	d
29	$B_4C_2D_1$	c,d	c,d	c,d	c,d	c,d	c,d	c,d	c,d	c,d	c,d	c,d	c,d	c	c,d	c,d	c,d
30	$B_4C_2D_2$	c,d	c,d	c,d	c,d	c,d	c,d	c,d	c,d	c,d	c,d	c,d	c,d	c	c,d	c,d	c,d
31	$B_4C_2D_3$	c,d	c,d	c,d	c,d	c,d	c,d	c,d	c,d	c,d	c,d	c,d	c,d	c,d	c,d	c,d	c,d
32	$B_4C_2D_4$	c,d	c,d	c,d	c,d	c,d	c,d	c,d	c,d	c,d	c,d	c,d	c,d	c,d	c,d	c,d	c,d

No	Ncv	17	18	19	20	21	22	23	24	25	26	27	28	29	30	31	32
1	$B_1C_1D_1$	a,b,c,d	a,b,c,d	a,b,c	a,b,c,d	a,b,c,d	a,b,c,d	a,b,c,d	a,b,c,d	a,b,c,d	a,b,c,d	a,b,c,d	a,b,c,d	a,b,c,d	a,b,c,d	a,b,c,d	a,b,c,d
2	$B_1C_1D_2$	a,b,c,d	a,b,c,d	a,b,c	a,b,c,d	a,b,c,d	a,b,c,d	a,b,c,d	a,b,c,d	a,b,c,d	a,b,c,d	a,b,c,d	a,b,c,d	a,b,c,d	a,b,c,d	a,b,c,d	a,b,c,d
3	$B_1C_1D_3$	c,d	a,b,c,d	a,b,c,d	c,d	a,b,c,d	a,b,c,d	a,b,c,d	a,b,c,d	a,b,c,d	a,b,c,d	a,b,c,d	a,b,c,d	a,b,c,d	a,b,c,d	a,b,c,d	a,b,c,d
4	$B_1C_1D_4$	c,d	c,d	a,c,d	c,d	b,c,d	c,d	a,b,c,d	a,b,c,d	a,b,c,d	a,b,c,d	a,c,d	a,b,c,d	c,d	c,d	a,b,c,d	a,b,c,d
5	$B_2C_1D_1$	b,c,d	a,b,c,d	a,b,c,d	a,b,c,d	a,b,c	a,b,c,d	a,b,c	a,b,c,d	a,b,c,d	a,b,c,d	a,b,c,d	a,b,c,d	a,b,c,d	a,b,c,d	a,b,c,d	a,b,c,d
6	$B_2C_1D_2$	c,d	a,b,c,d	a,b,c,d	a,b,c,d	a,b,c,d	a,b,c,d	a,b,c	a,b,c,d	a,b,c,d	a,b,c,d	a,b,c,d	a,b,c,d	a,b,c,d	a,b,c,d	a,b,c,d	a,b,c,d
7	$B_2C_1D_3$	c,d	a,b,c	a,b,c,d	c,d	a,b,c,d	a,b,c,d	a,b,c,d	a,b,c,d	a,b,c,d	a,b,c,d	a,b,c,d	a,b,c,d	a,b,c,d	a,b,c,d	a,b,c,d	a,b,c,d
8	$B_2C_1D_4$	c,d	a,b,c,d	a,b,c	c,d	a,b,c,d	a,b,c,d	a,b,c,d	a,b,c,d	a,c,d	a,c,d	a,b,c,d	a,b,c,d	a,b,c,d	a,b,c,d	a,b,c,d	a,b,c,d
9	$B_3C_1D_1$	a,c,d	c,d	c,d	c,d	c,d	a,b,c,d	b,c,d	a,b,c,d	c,d	a,c,d	a,b,c,d	a,c,d	a,c,d	c,d	b,c,d	a,b,c,d
10	$B_3C_1D_2$	c	c	c,d	c,d	c	c	c	c,d	c,d	c,d	c,d	a,c,d	c,d	c,d	c,d	c,d
11	$B_3C_1D_3$	c,d	c,d	c,d	c,d	c	c	c	c,d	c,d	c,d	c,d	a,c,d	c,d	c,d	c,d	c,d
12	$B_3C_1D_4$	c,d	c,d	c,d	c,d	c	c	c	c	d	c,d	c,d	c,d	c,d	c,d	c,d	c,d
13	$B_4C_1D_1$	c,d	c,d	c,d	c,d	d	c,d	a,b,c,d	a,c	c,d	c,d	c,d	c,d	c,d	c	b,c	a,b,c
14	$B_4C_1D_2$	c,d	c,d	c,d	c,d	c,d	c,d	c,d	c,d	c,d	c,d	c,d	c,d	-	c	c	c
15	$B_4C_1D_3$	c,d	c,d	c,d	c,d	c,d	c,d	d	d	c,d	c,d	c,d	c,d	d	c	c	c
16	$B_4C_1D_4$	c,d	c,d	c,d	c,d	c,d	c,d	c,d	c,d	c,d	c,d	c,d	c,d	d	c	c	c
17	$B_1C_2D_1$	–	c,d	c,d	c,d	c,d	c	c,d	c,d	c,d	c,d	a,c,d	b,c,d	c,d	c,d	c,d	a,b,c,d
18	$B_1C_2D_2$	c	–	c,d	c,d	c,d	c,d	c,d	c,d	c,d	c,d	c,d	c,d	c,d	c,d	c,d	c,d
19	$B_1C_2D_3$	d	d	–	c,d	c,d	c,d	c,d	c,d	c,d	c,d	c,d	c,d	c,d	c,d	c,d	c,d
20	$B_1C_2D_4$	d	c,d	d	–	c,d	c,d	c,d	c,d	c,d	c,d	c,d	c,d	c,d	c,d	c,d	a,b,c,d
21	$B_2C_2D_1$	c,d	c,d	c,d	c,d	–	c,d	c,d	c,d	c,d	c,d	c,d	a,c,d	c,d	c,d	c,d	c,d
22	$B_2C_2D_2$	c,d	c,d	c,d	c,d	c	–	c,d	c,d	c,d	c,d	c,d	c,d	c,d	c,d	c,d	c,d
23	$B_2C_2D_3$	c,d	c,d	c,d	c,d	c	c	–	c,d	c,d	c,d	c,d	c,d	d	c,d	c,d	c,d
24	$B_2C_2D_4$	c,d	c,d	c,d	c,d	c	c	-	–	c,d	c,d	c,d	c,d	d	c,d	c,d	c,d
25	$B_3C_2D_1$	c,d	c,d	c,d	c,d	c,d	c,d	c,d	c,d	–	c,d	c,d	c,d	c,d	c,d	c,d	c
26	$B_3C_2D_2$	c,d	c,d	c,d	c,d	c,d	d	c,d	c,d	c	–	c,d	c,d	c,d	c,d	c,d	c
27	$B_3C_2D_3$	c,d	c,d	c,d	c,d	c,d	c,d	c,d	d	c	c	–	c,d	c,d	c	c	c
28	$B_3C_2D_4$	c,d	c,d	c,d	c,d	c,d	c,d	c,d	c,d	c	c	c	–	c,d	c,d	c,d	c
29	$B_4C_2D_1$	c,d	c,d	c,d	c,d	c,d	c,d	c,d	c,d	c,d	c,d	c,d	c,d	–	c,d	c,d	c,d
30	$B_4C_2D_2$	c,d	c,d	c,d	c,d	c,d	c,d	c,d	c,d	c,d	c,d	c,d	c,d	c,d	–	c,d	c,d
31	$B_4C_2D_3$	c,d	c,d	c,d	c,d	c,d	c,d	c,d	c,d	c,d	c,d	c,d	c,d	c,d	c	–	c,d
32	$B_4C_2D_4$	c,d	c,d	c,d	c,d	c,d	c,d	c,d	c,d	c,d	c,d	c,d	c,d	c,d	c	c	–

Ncv – combination of research factors according to the scheme (Table 1); a,b,c,d – comparable pairs of variants with a significant difference in terms of F_0, F_{pl}, F_m and F_{st}, respectively (at the 95% family−wise confidence level).

Figure 9. Reliability of matching pairs of the combination of research factors according to Tukey HSD test.

In addition to a comprehensive assessment of the CFI curve parameters in oilseed radish, it is important to establish the variability of their fixation within a certain time period. Such an analysis was also important from the point of view of the predicted increasing value of the variation of the CFI curve indicators. According to Posudin et al. (2010), Guo & Tan (2015), Derks et al. (2015), Goltsev et al (2016), this is allowed to estimate and determine the internal variability of plant assimilation, determined, among

others, by agrotechnological factors of formation of agrocenosis of respective crop. Using basic variability parameters and mean error estimates (McDonald, 2014), we developed a graphical interpretation of the statistical evaluation of the CFI curve records (Figs 10–11). The formation of the mean values at each point of the instrumental fixation of the CFI curve indicators by a graphical interpretation of the standard deviation indicates a consistent increase of the standard error of the mean at the curve segment in the interval F_{pl}–F_m.

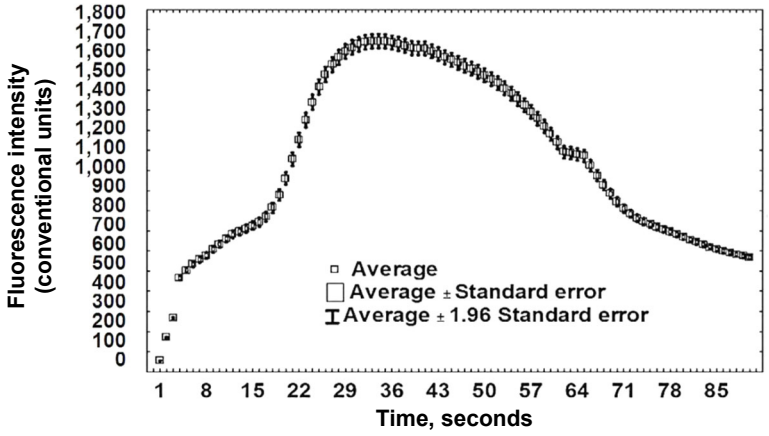

Figure 10. Graph of the average CFI curve of oilseed radish variety 'Zhuravka' in the average interval of different variants according to the combined general data 2015–2020.

The high values of the mean error retain their numerical values with some amplitude of oscillation until an intense decline towards the stationary fluorescence level F_{st}. This pattern of dynamic changes is confirmed by the graphical interpretation of the standard deviation of the CFI curve data (Fig. 11).

It should note that with increasing standard deviation and increasing total error of the mean, the oscillation coefficient indicates a low variation component in the CFI curve, namely the section covering the period from 23 to 41 seconds of recording, followed by a slow increase until the steady-state fluorescence F_{st} stage. The maximum values of the oscillation coefficient were recorded exactly in the F_0–F_{pl} interval. Similar results were obtained in Korneev (2002), Lamote et al. (2007), Brestic & Zivcak (2013), Ni et al. (2019), Khan et al. (2021), which observed the highest spreads of maximum fluorescence F_0 in different plant species within the reference group.

However, it is pointed out that in relation to the average, this deviation from the average does not form high rates of variation, unlike the sections of the CFI curve in the F_0–F_{pl} segment and the F_m–F_{st} segment. In contrast, studies (Flexas et al., 2002; Henriques, 2009; Bresson et al., 2015) showed and calculated minimal variation both in the F_0–F_{pl} sections and when reaching the F_{st} point.

The variable component of the basic indicators of the CFI curve is also determined by the hydrothermal conditions of the oilseed radish vegetation. This is confirmed by the results of the factor analysis in the ANOVAe estimation scheme of the experiment variants. It was determined that the share of influence of hydrothermal conditions of the year in the formation of the basic indicators of the CFI curve was in the range of

20.11–40.24%. Accordingly, the highest impact was for the F_{pl} indicator and the lowest for the F_0 indicator. Based on this, it was concluded that the indexes of the CFI curve depended on weather conditions, which additionally act as regulators of the positive or negative effect of the studied agrotechnological factors on the optimization of the post-sowing formation of the agrocenosis of oilseed radish.

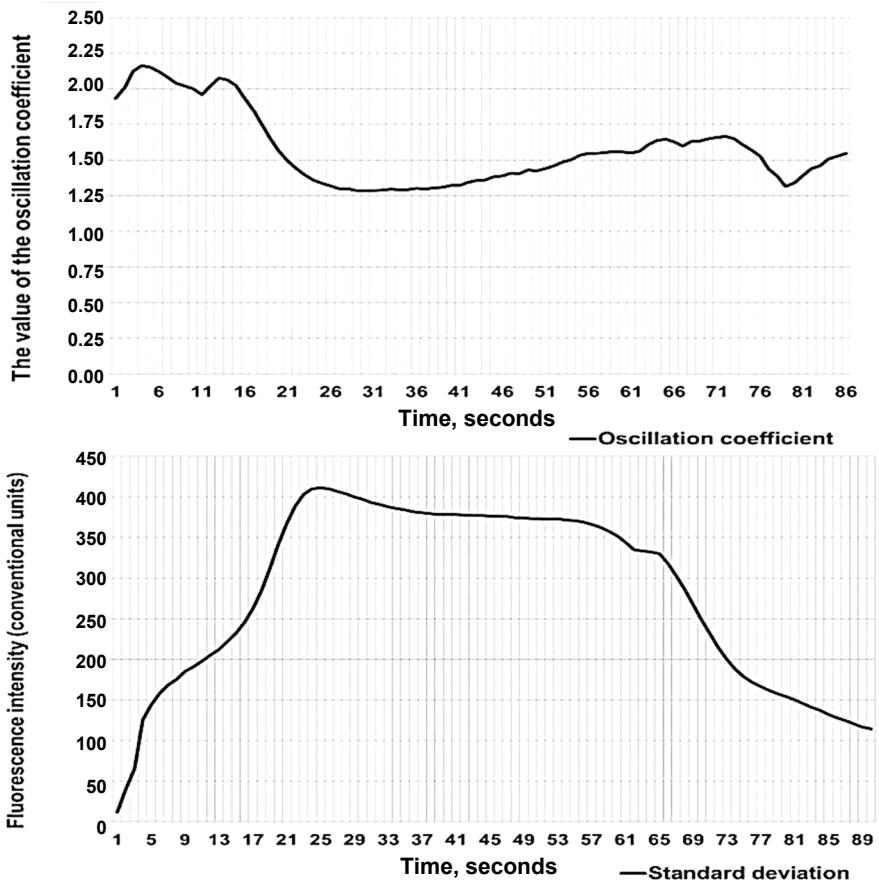

Figure 11. Statistical parameters of CFI curve of oilseed radish variety 'Zhuravka' in the average interval of different variants according to the combined general data 2015–2020.

As a result, generalizations made earlier on dynamic and complex nature of interrelations formation between the system of experience factors, basic indicative indices of CFI curve and indices of hydrothermal regime of environment during vegetation period of oilseed radish plants are shown by regression dependence data in Table 8 and Fig. 12. The obtained statistically reliable multiple regression coefficients indicated a sufficiently close dependence of complex combinatorial nature between the basic indicators of the CFI curve and agrotechnological factors in the system of experience variants. The established regression dependence in the equations of the second stage in accordance with Arkes (2019) indicates the presence of reciprocal extremes for the corresponding variants at the situational combination of factors in the system of dependencies.

Table 8. Regression dependences of the main indicators of the CFI curve on technological factors of oilseed radish agrocenosis design and the hydrothermal regime of the growing season (based on the data 2015–2020)

CFI curve indicator	Equation components x	Equation components y	Regression equation of dependence	Multiple regression coefficient R/ R^2	Statistical significance criteria R
F_0	Seeding rates, million germinable seeds ha^{-1}	Fertilizers in index expression	$F_0 = 416.0518+49.2454x-11.9687y-3.6012x^2+10.02xy+0.6562y^2$	0.942^{***} /0.887	$F/SS_{total} = 50.3$ ($p = .000000$), $t_{05} = 47.72$ ($p = 0.0000$)
F_{pl}			$F_{pl} = 697.68-48.956x+30.08y+9.6667x^2-3.2693xy-4y^2$	0.656^{***} /0.430	$F/SS_{total} = 10.96$ ($p = .000284$), $t_{05} = 75.20$ ($p = 0.0000$)
F_m			$F_{max} = 2102.9064-267.7319x+75.5537y+26.3274x^2-1.6253xy-9.2812y^2$	0.955^{***} /0.912	$F/SS_{total} = 65.86$ ($p = .0000000$), $t_{05} = 84.79$ ($p = 0.0000$)
F_{st}			$F_{st} = 443.7964+68.6235x-16.6312y-7.506x^2+12.9533xy+1.0937y^2$	0.895^{***} /0.801	$F/SS_{total} = 25.42$ ($p = .000000$), $t_{05} = 32.43$ ($p = 0.0000$)
F_0	Seeding rates, million germinable seeds ha^{-1}	Hydrothermal coefficient (HTC)	$F_0 = 638.4183-10.2759x-117.5909y-3.5268x^2+0.0414xy+37.9143y^2$	0.727^{***} /0.592	$F/SS_{total} = 48.48$ ($p = .000000$), $t_{05} = 113.85$ ($p = 0.0000$)
F_{pl}			$F_{pl} = 871.8071-62.8073x-166.7862y+10.8176x^2+3.9494xy+50.5807y^2$	0.425^{**} /0.180	$F/SS_{total} = 7.03$ ($p = .000001$), $t_{05} = 101.17$ ($p = 0.0000$)
F_m			$F_{max} = 1973.4387-253.3404x+106.552y+26.4603x^2-10.6975xy+13.4697y^2$	0.920^{***} /0.846	$F/SS_{total} = 238.4$ ($p = .000000$), $t_{05} = 118.46$ ($p = 0.0000$)
F_{st}			$F_{st} = 464.1891+94.6645x-14.6775y-7.5982x^2-3.8088xy-5.4553y^2$	0.885^{***} /0.783	$F/SS_{total} = 155.9$ ($p = .000000$), $t_{05} = 74.64$ ($p = 0.0000$)
F_0	Fertilizers in index expression	Hydrothermal coefficient (HTC)	$F_0 = 580.3522+24.1415x-117.4491y-3.9844x^2-0.0428xy+37.9143y^2$	0.349^{*} /0.121	$F/SS_{total} = 6.0$ ($p = .000005$), $t_{05} = 81.04$ ($p = 0.0000$)
F_{pl}			$F_{pl} = 776.5981+27.6075x-151.2187y-4.3944x^2-2.1312xy+48.1711y^2$	0.523^{**} /0.274	$F/SS_{total} = 12.0$ ($p = .000000$), $t_{05} = 105.0$ ($p = 0.0000$)
F_m			$F_{max} = 1554.5695+65.9432x+81.7799y-8.8646x^2+3.1428xy+13.4697y^2$	0.551^{**} /0.304	$F/SS_{total} = 18.8$ ($p = .000000$), $t_{05} = 49.76$ ($p = 0.0000$)
F_{st}			$F_{st} = 588.8348+8.8762x-20.623y+1.1198x^2-0.7973xy-5.4553y^2$	0.445^{**} /0.198	$F/SS_{total} = 10.7$ ($p = .000000$), $t_{05} = 49.77$ ($p = 0.0000$)

*, **, *** Significant at 5%, 1%, 0.1% level probability, respectively.

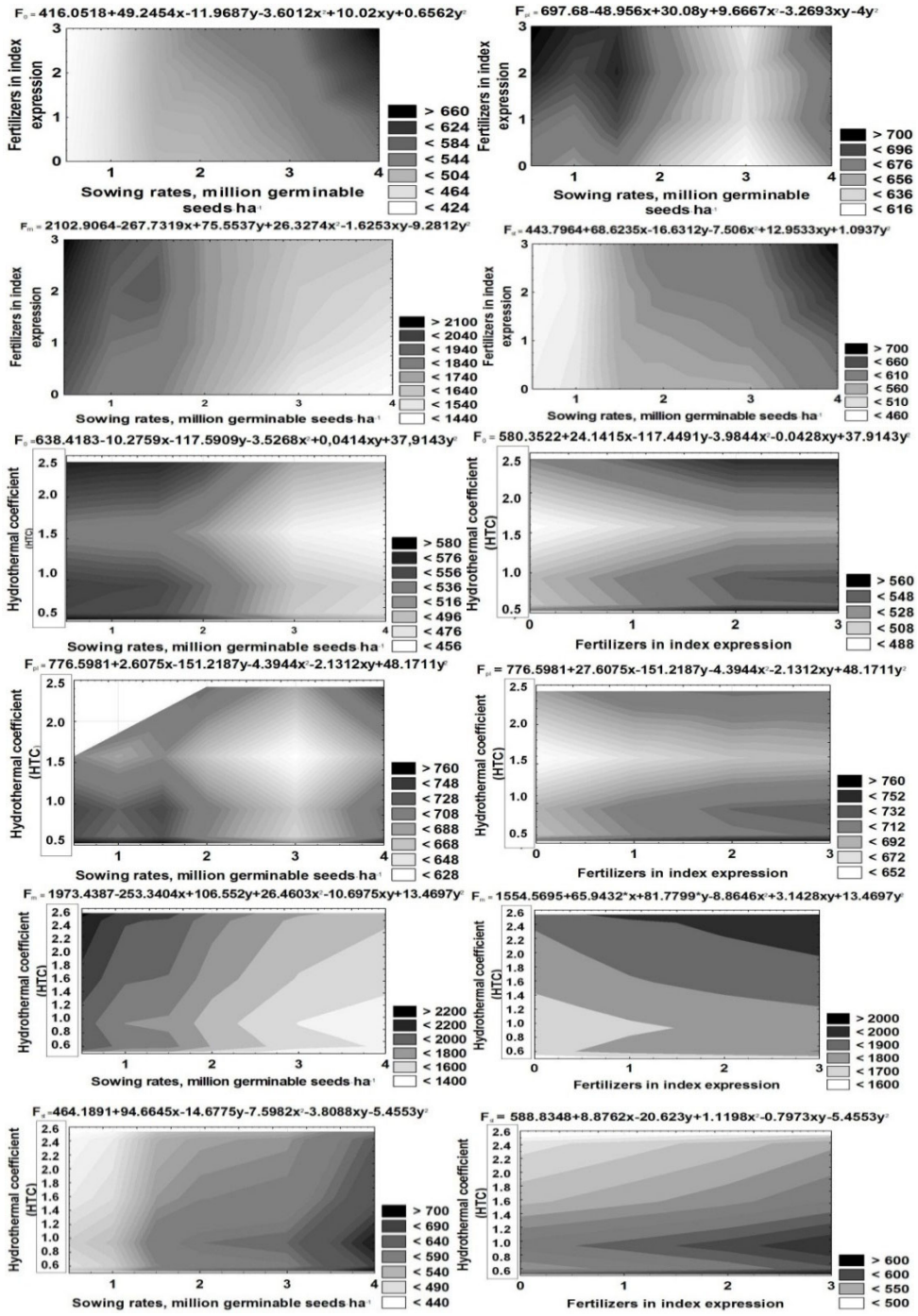

Consistently left and right dependencies for parameters: F_0, F_{pl}, F_m, F_{st}, F_0, F_0, F_{pl}, F_{pl}, F_m, F_m, F_{st}, F_{st}).

Figure 12. Projection surfaces of dependences of the main indicators of the CFI curve on technological factors of oilseed radish agrocenosis design and hydrothermal regime of vegetation (based on the 2015–2020 consolidated data set).

For all possible combinations in the regression scheme presented, the tightness of the multiple dependence on the basic criteria of the CFI curve in order of decreasing significance and approximation (according to R^2 criteria) with respect to experience and environmental factors can be placed in the following row: $F_m > F_{st} > F_0 > F_{pl}$. At the same time, the highest tightness of mutual influence on the formation of these indicators was noted for the use of seeding rates and fertilizer as influence factors, and, respectively, the lowest - for fertilizer and hydrothermal coefficient for the period from the beginning of the growing season to the date of recording the indicators of the CFI curve.

Thus, the confirmed stress role of fertilizers in the variants of increased seeding rates in interaction with the hydrothermal features of the environment complicates the nature of the direct expression of the impact both by combining the stress of a certain fraction of the influence of year conditions factors in the system of ANIOVA (Table 4), and by the dual role of fertilizers in a number of the variants studied (stimulation of growth - stress through increased competition in oilseed radish agrocenoses with with the smallest plant nutrition area).

As for the hydrothermal coefficient, to ensure the most harmonized CFI curve of oilseed radish plants, based on the nature of the reaction surfaces (Fig. 11) its value in the range 1.0–1.5 with tolerances from 0.8 to 1.7 is desirable to realize maximum crop bio-productivity of oiseed radish plant. It has been confirmed that this interval corresponds to the physiological desirability for optimising the growth and development of cruciferous crops (Hasanuzzaman, 2020; Bakhshandeh & Mohsen, 2021).

The reaction surfaces of the corresponding regression triads presented in Fig. 11 also allowed to identify the optimal variants for pre-sowing agro-technological construction of oilseed radish agrocenosis, which guarantee the harmonization of the basic indicators of the CFI curve in the study area and ensure the implementation of appropriate bioproductivity of 1 m^2 of sown area. Such agrotechnological parameters, taking into account the determined values of indicators F_0, F_{pl}, F_m and F_{st}, were the application of seeding rates in the interval of 1.0–2.0 million germinable seeds ha^{-1} (row sowing) and fertilization rate of $N_{30–60}P_{30–60}K_{30–60}$ and 1.5 million germinable seeds ha^{-1} (wide-row sowing) with a fertilization rate of $N_{60–90}P_{60–90}K_{60–90}$.

CONCLUSIONS

Thus, by the value of the main indices of the CFI curve F_0, F_{pl}, F_m, F_{st} and possible ratios, indices and coefficients calculated on their basis in comparison with such species as white mustard, spring bittercress and spring rape, oilseed radish should be considered as species with a wide range of adaptability to stress factors with a sensitive indicative response of the plant assimilative photosystem structures.

This allowed the application of the chlorophyll fluorescence induction method in the identification of optimal agro-technological solutions for its cultivation in order to maximise its photo-assimilative potential as a species.

Based on the results of the main recommended indicators in the analysis of the CFI curve within the studied options of pre-sowing design of oilseed radish agrocenosis by the parameters of row spacing, seeding rate and fertilizer application in the agro-climatic zone of research of such agricultural options: row sowing with seeding rate in the range of 1.0–2.0 million germinable seeds ha^{-1} with the fertilization rate of 30–60 kg N ha^{-1},

30–60 kg P ha^{-1}, and 30–60 kg K ha^{-1} and wide-row sowing with seeding rate of million germinable seeds ha^{-1} with the fertilization rate of 60–90 kg N ha^{-1}, 60–90 kg P ha^{-1}, and 60–90 kg K ha^{-1}.

Certain variants allowed to combine low values of F_0, and F_{st} parameters in comparison group at the level of 450–570 relative units of fluorescence with high values of maximum fluorescence (F_m) in the range of 1,700–2,000 relative units against the background of certain level of correlation dependence of direct and inverse character between the specified parameters and individual seed productivity of plants in the range of 0.560–0.992 ($p < 0.95$–0.99) and value of multiple regression coefficient between 0.349–0.955 ($p < 0.95$–0.99). This provided obtaining of appropriate indexes of CFI curve that certify both a sufficient leve of photoassimilative activity of oilseed radish plants and a high level of their viability. This made it possible to form a productive architecture of oilseed radish plants, which ensured the maximum seed yield among the studied variants.

REFERENCES

Amri, M., Abbes, Z., Trabelsi, I., Ghanem, M.E., Mentag, R. & Kharrat, M. 2021. Chlorophyll content and fluorescence as physiological parameters for monitoring *Orobanche foetida* Poir. infection in faba bean. *PLoS ONE* **16**(5), e0241527.

Arkes, J. 2019. *Regression Analysis A Practical Introduction*. 1st Edition. Routledge, 362 pp.

Arnetz, B.B. 1997. Technological stress: psychophysiological aspects of working with modern information technology. *Scandinavian Journal of Work, Environment & Health* **23**, 97–103.

Ashrostaghi, T., Aliniaeifard, S., Shomali, A., Azizinia, S., Abbasi Koohpalekani, J., Moosavi-Nezhad, M. & Gruda, N.S. 2022. The Role Player in Cucumber Response to Cold Stress. *Agronomy* **12**, 201.

Athar, H.U.R., Zafar, Z.U. & Ashraf, M. 2015. Glycinebetaine improved photosynthesis in canola under salt stress: evaluation of chlorophyll fluorescence parameters as potential indicators. *Journal of Agronomy and Crop Science* **201**, 428–442.

Ayyaz, A., Farooq, M.A., Dawood, M., Majid, A., Javed, M., Athar, H.U.R., Bano, H. & Zafar, Z.U. 2021. Exogenous melatonin regulates chromium stress-induced feedback inhibition of photosynthesis and antioxidative protection in Brassica napus cultivars. *Plant Cell Reports* **40**, 2063–2080.

Baba, W., Kompała-bąba, A., Zabochnicka-świątek, M., Luźniak, J., Hanczaruk, R., Adamski, A. & Kalaji, H.M. 2019. Discovering trends in photosynthesis using modern analytical tools: More than 100 reasons to use chlorophyll fluorescence. *Photosynthetica* **57**(2), 668–679.

Baker, N.R. & Rosenqvist, E. 2020 Applications of chlorophyll fluorescence can improve crop production strategies: an examination of future possibilities. *Journal of Experimental Botany* **71**(4), 1647.

Bakhshandeh, M.E. & Mohsen, J.J. 2021. Halothermal and hydrothermal time models describe germination responses of canola seeds to aging. *Plant Biology* **23**(4), 621–629.

Baldocchi, D.D., Ryu, Y., Dechant, B., Eichelmann, E., Hemes, K., Ma, S., Sanchez, C.R., Shortt, R., Szutu, D., Valach, A., Verfaillie, J., Badgley, G., Zeng, Y. & Berry, J.A. 2020. Outgoing near-infrared radiation from vegetation scales with canopy photosynthesis across a spectrum of function, structure, physiological capacity, and weather. *Journal of Geophysical Research: Biogeosciences* **125**, e2019JG005534.

Baležentienė, L. & Šiuliauskienė, D. 2007. Chlorophyll fluorescence estimation of fodder galega (*Galega orientalis* Lam.) in situ and dependence on different leaf rank and cultivars. *Agronomy Research* **5**(1), 3–12.

Björkman, O. & Demmig, B. 1987. Photon yield of O_2 evolution and chlorophyll fluorescence characteristics at 77 K among vascular plants of diverse origins. *Planta* **170**(4), 489–504.

Bonfig, K.B., Schreiber, U., Gabler, A., Roitsch, T. & Berger, S. 2006. Infection with virulent and avirulent P. syringae strains differentially affects photosynthesis and sink metabolism in Arabidopsis leaves. *Planta* **225**, 1–12.

Brack, W. & Frank, H. 1998. Chlorophyll a fluorescence: a tool for the investigation of toxic effects in the photosynthetic apparatus. *Ecotox-icology and Environmental Safety* **l40**(1–2), 34–41.

Bresson, J., Vasseur, F., Dauzat, M., Koch, G., Granier, C. & Vile, D. 2015. Quantifying spatial heterogeneity of chlorophyll fluorescence during plant growth and in response to water stress. *Plant methods* **11**, 23.

Brestič, M., Živčák, M., Kalaji, H.M., Carpentier, R. & Allakhverdiev, S.I. 2012. Photosystem II thermostability in situ: Environmentally induced acclimation and genotype-specific reactions in *Triticum aestivum* L. *Plant Physiology and Biochemistry* **57**, 93–105.

Brestic, M & Zivcak, M. 2013. PSII fluorescence techniques for measurement of drought and high temperature stress signal in plants: protocols and applications. In: *Rout GR, Das AB (eds.) Molecular stress physiology of plants*. Springer Dordrecht, 87–131.

Brion, O.V., Korneev, D.Yu., Snegur, O.I. & Kitaev, O.O. 2000. *Instrumental study of the photosynthetic apparatus by induction of chlorophyll fluorescence: Guidelines for students of the Faculty of Biology*. Kyiv: Kyiv University Publishing and Printing Center, 15 pp. (in Ukrainian).

Bukhat, S., Manzoor, H., Zafar, Z.U., Azeem, F. & Rasul, S. 2020. Salicylic acid induced photosynthetic adaptability of Raphanus sativus to salt stress is associated with antioxidant capacity. *Journal of Plant Growth Regulation* **39**, 809–822.

Burling, K., Hunsche, M. & Noga, G. 2011. Use of blue-green and chlorophyll fluorescence measurements for differentiation between nitrogen deficiency and pathogen infection in winter wheat. *Journal of Plant Physiology* **168**, 1641–1648.

Bussotti, F., Gerosa, G., Digrado, A. & Pollastrini, M. 2020. Selection of chlorophyll fuorescence parameters as indicators of photosynthetic efciency in large scale plant ecological studies. *Ecological Indicators* **108**, 105686.

Casto, A., Schuhl, H., Schneider, D., Wheeler, J., Gehan, M. & Fahlgren, N. 2021. Analyzing chlorophyll fluorescence images in PlantCV PT. *Earth and Space Science*, AID 10.1002/essoar.10508322.2.

Cendrero-Mateo, M.P., Wieneke, S., Damm, A., Alonso, L., Pinto, F., Moreno, J., Guanter, L., Celesti, M., Rossini, M., Sabeter, N., Cogliati, S., Julitta, T., Rascher, U., Goulas, Y., Aasen, H., Pacheco-Labrador, J. & Arthur, A.M. 2019. Sun-Induced Chlorophyll Fluorescence III: Benchmarking Retrieval Methods and Sensor Characteristics for Proximal Sensing. *Remote Sensing* **11**, 962.

Cetner, M.D., Kalaji, H.M., Goltsev, V., Aleksandrov, V., Kowalczyk, K., Borucki, W. & Jajoo, A. 2017. Effects of nitrogendeficiency on efficiency of light-harvesting apparatus in radish. *Plant Physiology and Biochemistry* **119**, 81–92.

Christen, D., Schonmann, S., Jermini, M., Strasser, R.J. & Défago, G. 2007. Characterization and early detection of grapevine (*Vitis vinifera*) stress responses to esca disease by in situ chlorophyll fluorescence and comparison with drought stress. *Environmental and Experimental Botany* **60**, 504–514.

Cong, W., Yang, K. & Wang, F. 2022. Canopy Solar-Induced Chlorophyll Fluorescence and Its Link to Transpiration in a Temperate Evergreen Needleleaf Forest during the Fall Transition. *Forests* **13**, 74.

Cui, X., Tang, Y., Gu, S., Nishimura, S., Shi, S. & Zhao, X. 2003. Photosynthetic depression in relation to plant architecture in two alpine herbaceous species. *Environmental and experimental botany* **50**(2), 125–135.

De Canniére, S. & Jonard, F. 2021. Tracking Water Limitation in Photosynthesis with Sun-Induced Chlorophyll Fluorescence. 2021 *IEEE International Geoscience and Remote Sensing Symposium IGARSS*, 6367–6370.

Dechant, B., Ryu, Y., Badgley, G., Zeng, Y., Berry, J.A., Zhang, Y., Goulas, Y., Li, Z., Zhang, Q., Kang, M., Li, J. & Moya, I. 2020. Canopy structure explains the relationship between photosynthesis and sun-induced chlorophyll fluorescence in crops. *Remote Sensing of Environment* **241**, 111733.

Derks, A., Schaven, K. & Bruce, D. 2015. Diverse mechanisms for photoprotection in photosynthesis. Dinamic regulation of photosystem II excitation in response to rapin environmental change. *Biochimica et Biophysica Acta – Bioenergetics* **1847**(4–5), 468–485.

Driever, S., Lawson, T., Andralojc, P., Raines, C. & Parry, M. 2014. Natural variation in photosynthetic capacity, growth, and yield in 64 field-grown wheat genotypes. *Journal of Experimental Botany* **65** (17), 4959–4973.

Evans, J.R. 2009. Potential errors in electron transport rates calculated from chlorophyll fluorescence as revealed by a multilayer leaf model. *Plant and Cell Physiology* **50**, 698–706.

Evarte-Bundere, G. & Evarts-Bunders, P. 2012. Using of the Hydrothermal coefficient (HTC) for interpretation of distribution of non-native tree species in Latvia on example of cultivated species of genus Tilia. *Acta Biologica Universitatis Daugavpiliensis* **12**, 135–148.

Feria-Gómez, D.F., Londoño-Puerta, D.A. & Córdoba-Gaona, O. de J. 2022. Relationship between the chlorophyll a fluorescence and the yield in banana (Musa AAA Simmonds cv. Cavendish). *Revista Colombiana de Ciencias Hortícolas* **16**(1), e13313.

Ferreira, L.C., Moreira, B.R.A., Montagnolli, R.N., Prado, E.P., Viana, R.D.S., Tomaz, R.S., Cruz, J.M., Bidoia, E.D., Frias, Y.A. & Lopes, P.R.M. 2021. Green Manure Species for Phytoremediation of Soil With Tebuthiuron and Vinasse. *Frontiers in Bioengineering and Biotechnology* **8**, 613–642.

Flexas, J., Escalona, J.M., Evain, S., Gulías, J., Moya, I., Osmond, C.B. & Medrano, H. 2002. Steady-state chlorophyll fluorescence (Fs) measurements as a tool to follow variations of net CO_2 assimilation and stomatal conductance during water-stress in C3 plants. *Physiologia Plantarum* **114**(2), 231–240.

Flexas, J., Bota, J., Loreto, F., Cornic, G. & Sharkey, T.D. 2004. Diffusive and metabolic limitations to photosynthesis under drought and salinity in C3 plants. *Plant Biology* **6**, 269–279.

Gensheimer, J., Turner, A.J., Köhler, P., Frankenberg, C. & Chen, J. 2022. A convolutional neural network for spatial downscaling of satellite-based solar-induced chlorophyll fluorescence (SIFnet). *Biogeosciences* **19**, 1777–1793.

Goltsev, V.N., Kaladzhi, M.Kh., Kuzmanova, M.A. & Allakhverdiev, S.I. 2014. *Variable and delayed fluorescence of chlorophyll a – theoretical foundations and practical applications in plant research*. Moscow-Izhevsk: Institute for Computer Research. 220 pp. (in Russian).

Goltsev, V.N., Kalaji, H.M., Paunov, M. & Baba, W. 2016. Variable chlorophyll fluorescence and its use for assessing physiological condition of plant photosynthetic apparatus. *Russian Journal of Plant Physiology* **63**, 869–893.

Gu, J., Zhou, Z., Li, Z., Chen, Y., Wang, Z., Zhang, H. & Yang, J. 2017. Photosynthetic properties and potentials for improvement of photosynthesis in pale green leaf rice under high light conditions. *Frontiers in Plant Science* **8**, 1082.

Guidi, L., Lo Piccolo, E. & Landi, M. 2019. Chlorophyll Fluorescence, Photoinhibition and Abiotic Stress: Does it Make Any Difference the Fact to Be a C3 or C4 Species? *Frontiers in Plant Science* **10**,174.

Guo, Y.P., Guo, D.P., Zhaoa, J.P., Liua, H., Penga, Y., Wanga, Q.M., Chenb, J.S. & Rao, G.Z. 2005. Photosynthetic responses of radish (*Raphanus sati*vus var. *longipinnatus*) plants to infection by turnip mosaic virus. *Photosynthetica* **43**, 457–462.

Guo, Y. & Tan, J. 2015. Recent advances in the application of chlorophyll a fluorescence from Photosystem II. Photochem. *Photobiology* **91**, 1–14.

Guo, X., Li, G., Ding, X., Zhang, J., Ren, B., Liu, P., Zhang, S. & Zhao, B. 2022. Response of Leaf Senescence, Photosynthetic Characteristics, and Yield of Summer Maize to Controlled Release Urea-Based Application Depth. *Agronomy* **12**, 687.

Gururani, M.A., Venkatesh, J. & Tran, L.S.P. 2015. Regulation of photosynthesis during abiotic stress-induced photoinhibition. *Molecular Plant* **8**, 1304–1320.

Hamann, F.A. 2021. *Potential and limitations for the practical use of fluorescence sensors to detect physiological adaptations of crops*. PhD Thesis. Bonn. Institute for Crop Science and Resource Conservation, 116 pp.

Hasanuzzaman, M. 2020. *The Plant Family Brassicaceae Biology and Physiological Responses to Environmental Stresses*. Springer, Singapore. 531 pp.

He, J., Chee, C.W. & Goh, C.J. 1996. 'Photoinhibition' of Heliconia under natural tropical conditions: the importance of leaf orientation for light interception and leaf temperature. *Plant, Cell & Environment* **19**(11), 1238–1248.

Henriques, F.S. 2009. Leaf Chlorophyll Fluorescence: Background and Fundamentals for Plant Biologists. *Botanical Review* **75**, 249–270.

Herritt, M.T., Long, J.C., Roybal, M.D., Moller Jr, D.C., Mockler, T.C., Pauli, D. & Thompson, A.L. 2021. FLIP:FLuorescence imaging pipeline for field-based chlorophyll fluorescence images. *SoftwareX*. **14**, Article 100685.

Herritt, M.T., Pauli, D., Mockler, T.C. & Thompson, A.L. 2020. Chlorophyll fluorescence imaging captures photochemical efficiency of grain sorghum (*Sorghum bicolor*) in a field setting. *Plant Methods* **16**, 109.

Hosseinzadeh, M., Aliniaeifard, S., Shomali, A. & Didaran, F. 2021. Interaction of light intensity and CO_2 concentration alters biomass partitioning in Chrysanthemum. *Journal of Horticultural Research* **29**, 45–56.

Hou, W.H., Zhang, Y.X., Wang, H.J., Zhang, Q.X., Hou, M.L., Cong, B.M. & Du, X. 2021. Effects of nitrogen application level on leaf photosynthetic characteristics and chlorophyll fluorescence characteristics of *Leymus chinensis*. *Acta Agrestia Sinica* **29**, 532–536.

Hupp, S., Rosenkranz, M., Bonfig, K., Pandey, C. & Roitsch, T. 2019. Noninvasive Phenotyping of Plant-Pathogen Interaction: Consecutive In Situ Imaging of Fluorescing Pseudomonas syringae, Plant Phenolic Fluorescence, and Chlorophyll Fluorescence in Arabidopsis Leaves. *Frontiers in Plant Science* **10**, 1239.

IUSS Working Group. 2015. *WRB: World Reference Base for Soil Resources. World Soil Resources Reports* 106. FAO. Rome, pp. 85–90.

Jamil, M. & Rha, E. 2013. NaCl Stress-Induced Reduction in Grwoth, Photosynthesis and Protein in Mustard. *Journal of Agricultural Science* **5**(9), 114–127.

Janušauskaite, D. & Feiziene, D. 2012. Chlorophyll fluorescence characteristics throughout spring triticale development stages as affected by fertilization. *Acta Agriculturae Scandinavica, Section B*. *Soil and Plant Science* **62**, 7–15.

Javed, M., Ashraf, M., Iqbal, M., Farooq, M.A., Zafar, Z.U. & Athar, H.-ur-R. 2022. Chlorophyll fluorescence, ion uptake, and osmoregulation are potential indicators for detecting ecotypic variation in salt tolerance of Panicum antidotale Retz. *Arid Land Research and Management* **36**(1), 84–108.

Jedmowski, C., Ashoub, A., Momtaz, O.A., & Brüggemann, W. 2015. Impact of Drought, Heat, and Their Combination on Chlorophyll Fluorescence and Yield of Wild Barley (*Hordeum spontaneum*). *Journal of Botany*. Article ID 120868, 1–9.

Jonathan, M.B. 2017. Continuous excitation chlorophyll fluorescence parameters: a review for practitioners. *Tree Physiology* **37**(8), 1128–1136.

Kalaji, H.M., Jajoo, A., Oukarroum, A. & Brestic, M. 2016. Chlorophyll a fluorescence as a tool to monitor physiological status of plants under abiotic stress conditions. *Acta Physiologiae Plantarum* **38**, 102–114.

Kalaji, H., Schansker, G., Ladle, R., Goltsev, V., Bosa, K., Allakhverdiev, S., Brestic, M., Bussotti, F. & Calatayud, A. 2014. Frequently asked questions about in vivo chlorophyll fluorescence: practical issues. *Photosynthesis Research* **122**, 121–158.

Kalaji, H.M., Schansker, G., Brestic, N., Bussotti, F., Calatayud, A., Ferroni, L. & Goltsev, V. 2017. Frequently asked questions about chlorophyll fluorescence, the sequel. *Photosynthesis Research* **132**, 13–66.

Kalaji, H.M., Bąba, W., Gediga, K., Goltsev, V., Samborska, I., Cetner, M.D., Dimitrova, S., Piszcz, U., Bielecki, K., Karmowska, K., Dankov, K. & Kompała-Bąba, A. 2017a. Chlorophyll fluorescence as a tool for nutrient status identification in rapeseed plants. *Photosynthesis Research* **136**, 329–343.

Kalaji, H.M., Goltsev, V.N., Żuk-Golaszewska, K., Zivcak, M. & Brestic, M. 2017b. *Chlorophyll Fluorescence. Understanding Crop Performance: Basics and Applications*. CRC Press, Boca Raton, 222 pp.

Kalaji, H.M., Bąba, W., Gediga, K., Goltsev, V., Samborska, I.A., Cetner, M.D., Dimitrova, S., Piszcz, U., Bielecki, K., Karmowska, K., Dankov, K. & Kompała-Bąba, A. 2018. Chlorophyll fluorescence as a tool for nutrient status identification in rapeseed plants. *Photosynthesis Research* **136**(3), 329–343.

Kaletnik, G., Pryshliak, N. & Tokarchuk, D. 2021. Potential of production of energy crops in Ukraine and their processing on solid biofuels. *Ecological Engineering and Environmental Technology* **22**(3), 59–70.

Kaletnik, G., Honcharuk, I. & Okhota, Y. 2020. The Waste-free production development for the energy autonomy formation of Ukrainian agricultural enterprises. *Journal of Environmental Management and Tourism* **11**(3), 513–522.

Kayaçetin, F. 2020. Botanical characteristics, potential uses, and cultivation possibilities of mustards in turkey: A review. *Turkish Journal of Botany* **44**, 101–127.

Keller, B., Matsubara, S., Rascher, U., Pieruschka, R., Steier, A., Kraska, T. & Muller, O. 2019. Genotype specific photosynthesis × environment interactions captured by automated fluorescence canopy scans over two fluctuating growing seasons. *Frontiers in Plant Science* **10**, 1482.

Khan, N., Essemine, J., Hamdani, S., Qu, M., Lu, M.-J.A., Parveen, S., Stirbet, A., Govindjee, G. & Zhu, X.-G. 2021. Natural variation in the fast phase of chlorophyll a fluorescence induction curve (OJIP) in a global rice minicore panel. *Photosynthesis Research* **150**(1–3), 137–158.

Kim, J., Ryu, Y., Dechant, B., Lee, H., Kim, H.S., Kornfeld, A. & Berry, J.A. 2021 Solar-induced chlorophyll fluorescence is non-linearly related to canopy photosynthesis in a temperate evergreen needleleaf forest during the fall transition *Remote Sensing of Environment* **258**, 112362.

Kimm, H., Guan, K., Burroughs, C.H., Peng, B., Ainsworth, E.A., Bernacchi, C.J., Moore, C.E., Kumagai, E., Yang, X., Berry, J.A. & Wu, G. 2021. Quantifying high-temperature stress on soybean canopy photosynthesis: the unique role of sun-induced chlorophyll fluorescence. *Global Change Biology* **27**, 2403–2415.

Kirik, M.M., Taranuho & Yu.M. 2011. Diagnosis of viral infection of black currant and raspberry by the method of induction of chlorophyll fluorescence of leaves. *Bulletin of Agrarian Science: Coll. Science. works* **10**, 26–28 (in Ukrainian).

Korneev, D.Yu. 2002. *Informational capabilities of the method of chlorophyll fluorescence induction*. Kiev: Alterpress. 188 pp. (in Ukrainian).

Kuhlgert, S., Austic, G., Zegarac, R., Osei-Bonsu, I., Hoh, D., Chilvers, M.I., Roth, M.G., Bi, K., TerAvest, D. & Weebadde, P. 2016. MultispeQ Beta: a tool for large-scale plant phenotyping connected to the open PhotosynQ network. *Royal Society Open Science* **3**(10), 160592.

Lamote, M., Johnson, L.E. & Lemoine, Y. 2007. Interspecific differences in the response of juvenile stages to physical stress: fluorometric responses of fucoid embryos to variation in meteorological conditions. *Journal of Phycology* **43**(6), 1164–1176.

Larouk, C., Gabon, F., Kehel, Z., Djekoun, A., Nachit, M. & Amri, A. 2021. Chlorophyll Fluorescence and Drought Tolerance in a Mapping Population of Durum Wheat. *Contemporary Agriculture* **70**(3–4), 123–134.

Legendre, R., Basinger, N.T. & van Iersel, M.W. 2021. Low-Cost Chlorophyll Fluorescence Imaging for Stress Detection. *Sensors* **21**(6), 2055.

Lei, S., Xiping, D. & Li, Y. 2006. Effects of water deficit on fluorescence parameters of wheat with different ploidies. *Xibei Zhiwu Xuebao* **26**(2), 343–347.

Li, Z., Zhang, Q., Li, J., Yang, X., Wu, Y., Zhang, Z., Wang, S., Wang, H. & Zhang, Y. 2020. Solar-induced chlorophyll fluorescence and its link to canopy photosynthesis in maize from continuous ground measurements *Remote Sensing of Environment* **236**, 111420.

Lichtenthaler, H.K., Buschmann, C. & Knapp, M. 2005. How to Correctly Determine the Different Chlorophyll Fluorescence Parameters and the Chlorophyll Fluorescence Decrease Ratio RFd of Leaves with the PAM Fluorometer. *Photosynthetica* **43**, 379–393.

Lin, J., Shen, Q., Wu, J., Zhao, W. & Liu, L. 2022. Assessing the Potential of Downscaled Far Red Solar-Induced Chlorophyll Fluorescence from the Canopy to Leaf Level for Drought Monitoring in Winter Wheat. *Remote Sensing* **14**, 1357.

Liu, L., Guan, L. & Liu, X. 2017. Directly estimating diurnal changes in GPP for C3 and C4 crops using far-red sun-induced chlorophyll fluorescence. *Agricultural and Forest Meteorology* **232**, 1–9.

Logan, B.A., Demmig-Adams, B., Adams, W.W. & Bilger, W. 2014. Context, quantification, and measurement guide for non-photochemical quenching of chlorophyll fluorescence, in *Non-Photochemical Quenching and Energy Dissipation in Plants, Algae and Cyanobacteria*, eds B. Demmig-Adams, G. Garab, W.W. Adams, Govindjee (Dordrecht: Springer), pp. 187–201.

Lootens, P., Van Waes, J. & Carlier, L. 2004. Effect of a short photoinhibition stress on photosynthesis, chlorophyll a fluorescence, and pigment contents of different maize cultivars. can a rapid and objective stress indicator be found? *Photosynthetica* **42**, 187–192.

Magney, T.S., Barnes, M.L. & Yang, X. 2020. On the covariation of chlorophyll fluorescence and photosynthesis across scales. *Geophysical Research Letters* **47**, e2020GL091098.

Maguire, A.J., Eitel, J.U.H., Griffin, K.L., Magney, T.S., Long, R.A., Vierling, L.A., Schmiege, J.S., Jennewein, W.A., Weygint, N.T. & Bruner, B.S.G. 2020. On the functional relationship between fluorescence and photochemical yields in complex evergreen needleleaf canopies. *Geophysical Research Letters* **47**, e2020GL087858.

Mathur, S., Agrawal, D. & Jajoo, A. 2014. Photosynthesis: Responses to High Temperature Stress. *Journal of Photochemistry and Photobiology* **137**, 116–126.

Maxwell, K. & Johnson, G.N. 2000. Chlorophyll fuorescence – a practical guide. *Journal of Experimental Botany* **51**(345), 659–668.

McAusland, L., Atkinson, J.A., Lawson, T. & Murchie, E.H. 2019. High throughput procedure utilising chlorophyll fluorescence imaging to phenotype dynamic photosynthesis and photoprotection in leaves under controlled gaseous conditions. *Plant Methods* **15**, 109.

McDonald, J.H. 2014. *Handbook of Biological Statistics*, 3rd ed. Sparky House Publishing, Baltimore, Maryland. 291 pp.

Moore, C.E., Meacham-Hensold, K., Lemonnier, P., Slattery, R.A., Benjamin, C., Bernacchi, C.J., Lawson, T. & Cavanagh, A.P. 2021. The effect of increasing temperature on crop photosynthesis: from enzymes to ecosystems. *Journal of Experimental Botany* **72**(8), 2822–2844.

Murata, N., Takahashi, S., Nishiyama, S. & Allakhverdiev, S.I. 2007. Photoinhibition of photosystem II under environmental stress. *Biochimica et Biophysica Acta* **1767**, 414–421.

Murchie, E.H., Kefauver, S., Araus, J.L., Muller, O., Rascher, U., Flood, P.J. & Lawson, T. 2018. Measuring the dynamic photosynthome. *Annals of Botany* **122**(2), 207–220.
Murchie, E.H. & Lawson, T. 2013. Chlorophyll fluorescence analysis: a guide to good practice and understanding some new applications. *Journal of Experimental Botany* **64**, 3983–3998.
Naidu, S.L. & Long, S.P. 2004. Potential mechanisms of low-temperature tolerance of C4 photosynthesis in Miscanthusgiganteus: an in vivo analysis. *Planta* **220**, 145–155.
Nesterenko, T.V., Tikhomirov, A.A. & Shikhov, V.N. 2006. Ontogenetic approach to the assessment of plant resistance to prolonged stress using chlorophyll fluorescence induction method. *Photosynthetica* **44**(3), 321–332.
Nesterenko, T.V., Tikhomirov, A.A. & Shikhov, V.N. 2012. Influence of excitation light intensity and leaf age on the slow chlorophyll fluorescence transiet in radish. *Biophysics* **57**(4), 614–620 (in Russian).
Ni, Z., Lu, Q., Huo, H. & Zhang, H. 2019. Estimation of Chlorophyll Fluorescence at Different Scales: A Review. *Sensors* **19**(13), 1–22.
Oláh, V., Hepp, A., Irfan, M. & Mészáros, I. 2021. Chlorophyll Fluorescence Imaging-Based Duckweed Phenotyping to Assess Acute Phytotoxic Effects. *Plants* **10**, 2763.
Østrem, L., Rapacz, M., Larsen, A., Marum, P. & Rognli, O.A. 2018. Chlorophyll a Fluorescence and Freezing Tests as Selection Methods for Growth Cessation and Increased Winter Survival in ×Festulolium. *Frontiers in Plant Science* **9**, 1200.
Pérez-Bueno, M.L., Pineda, M. & Barón, M. 2019. Phenotyping plant responses to biotic stress by chlorophyll fluorescence imaging. *Frontiers in Plant Science* **10**, 1135.
Petjukevics, A. & Skute, N. 2022. Chlorophyll fluorescence changes, as plant early state indicator under different water salinity regimes on invasive macrophyte *Elodea canadensis* (Michx., 1803). *ARPHA Preprints*, e82408.
Portable fluorometer 'Floratest': Operating instructions. Institute of Cybernetics of V.M. Elushkova NAS of Ukraine, 2011. 27 pp. (in Ukraine).
Porcar-Castell, A., Malenovský, Z., Magney, T., Van Wittenberghe, S., Fernández-Marín, B., Maignan, F., Zhang, Y., Maseyk, K., Atherton, J., Albert, L.P., Robson, T.M., Zhao, F., Garcia-Plazaola, J.-I., Ensminger, I., Rajewicz, P.A., Grebe, S., Tikkanen, M., Kellner, J.R., Ihalainen, J.A., Rascher, U. & Logan, B. 2021. Chlorophyll a fluorescence illuminates a path connecting plant molecular biology to Earth-system science. *Natural Plants* **7**, 998–1009.
Posudin, Y.I., Godlevska, O.O., Zaloilo, I.A. & Kozhem'yako, Ya.V. 2010. Application of portable fluorometer for estimation of plant tolerance to abiotic factors. *Agrophysics* (**24**)4, 363–368.
Posudin, Y.I. & Bogdasheva, O.V. 2010. Fluorescent analysis of pea sown Pisum sativum during development and under the influence of external factors. *Scientific reports of National University of Life and Environmental Sciences of Ukraine* **5**(21), 123–128 (in Ukrainian).
Rao, L., Li, S. & Cui, X. 2021. Leaf morphology and chlorophyll fluorescence characteristics of mulberry seedlings under waterlogging stress. *Scientific Reports* **11**, 13379.
Raza, M.A.S., Shahid, A.M., Saleem, M.F., Khan, I.H., Ahmad, S., Ali, M. & Iqbal, R. 2017. Effects and management strategies to mitigate drought stress in oilseed rape (*Brassica napus* L.): a review. *Zemdirbyste-Agriculture* **104**(1), 85–94.
Rintamäki, E., Salo, R., Lehtonen, E. & Aro, E.-M. 1995. Regulation of D1-protein degradation during photoinhibition of photosystem II *in vivo*: Phosphorylation of the D1 protein in various plant groups. *Planta* **195**(3), 379–386.
Roháček, K. 2002. Chlorophyll fluorescence parameters: the definitions, photosynthetic meaning, and mutual relationships. *Photosynthetica* **40**, 13–29.
Romanov, V.O., Artemenko, D.M. & Braiko, Y.O. 2011. Family of portable devices 'Floratest': preparation for serial production. *Computer tools, networks and systems* **10**, 85–93.

Romanov, V.O., Starodub, M.F. & Galelyuka, I.B. 2010. Biosensors for express-diagnostics of photosynthesis and acute viral infections. *Proceedings: Measurements Control Computers in Economy and Environment Protection* **3**, 3–7.

Ruban, A.V. 2016. Nonphotochemical chlorophyll fluorescence quenching: mechanism and effectiveness in protecting plants from photodamage. *Plant Physiology* **170**, 1903–1916.

Ruban, A.V. & Murchie, E.H. 2012. Assessing the photoprotective effectiveness of non-photochemical chlorophyll fluorescence quenching: a new approach. *Biochimica et Biophysica Acta* **1817**, 977–982.

Rumsey, D.J. 2016. *Statistics for Dummies*. 2nd Edition. John Wiley & Sons Inc. 408 pp.

Sarahan, E.V. 2011. Features of practical application of portable biosensor devices of the 'Floratest' family. *Computer tools, networks and systems* **10**, 94–103 (in Ukrainian).

Schreiber, U., Hormann, H., Neubauer, C. & Klughammer, C. 1995. Assessment of photosystem II photochemical quantum yield by chlorophyll fluorescence quenching analysis. *Functional Plant Biology* **22**, 209–220.

Schreiber, U. & Klughammer, C. 2013. Wavelength-dependent photodamage to Chlorella investigated with a new type of multi-color PAM chlorophyll fluorometer. *Photosynthesis Research* **114**, 165–177.

Schreiber, U. & Klughammer, C. 2021. Evidence for variable chlorophyll fluorescence of photosystem I in vivo. *Photosynthesis Research* **149**, 213–231.

Schuback, N., Tortell, P.D., Berman-Frank, I., Campbell, D.A., Ciotti, A., Courtecuisse, E., Erickson, Z.K., Fujiki, T., Halsey, K., Hickman, A.E., Huot, Y., Gorbunov, M.Y., Hughes, D.J., Kolber, Z.S., Moore, C.M., Oxborough, K., Prášil, O., Robinson, C.M., Ryan-Keogh, T.J. & Varkey, D.R. 2021. Single-turnover variable chlorophyll fluorescence as a tool for assessing phytoplankton photosynthesis and primary productivity: opportunities, caveats and recommendations. *Frontiers in Marine Science* **8**, 1–24, 690607.

Selyaninov, G.L. 1928. About the agricultural evaluation of the climate. *Trudy GGO* **20**, 177–185 (in Russian).

Sepúlveda, P.M. & Johnstone, D. 2019. A Novel Way of Assessing Plant Vitality in Urban Trees. *Forests*. **10** (1), 2.

Shomali, A. & Aliniaeifard, S. 2020. Overview of signal transduction in plants under salt and drought stresses. In *Salt and Drought Stress Tolerance in Plants*. Springer: Berlin/Heidelberg, Germany, pp. 231–258.

Shpaar, D. 2012. *Rapeseed and colza: cultivation, harvesting, use*. Publisher: Zerno, 368 pp.

Simeneh, T.A. 2020. Photosynthesis limiting stresses under climate change scenarios and role of chlorophyll fluorescence. *Cogent Food & Agriculture* **6**, 1–18.

Sinyagin, I.I. 1975. *Plant nutrition areas*. Moscow, Rosselkhozizdat, 383 pp. (in Russian).

Sloat, L.L., Lin, M., Butler, E.E., Johnson, D., Holbrook, N.M., Huybers, P.J., Lee, J.E. & Mueller, N.D. 2021. Evaluating the benefits of chlorophyll fluorescence for in-season crop productivity forecasting. *Remote Sensing of Environment* **260**, 112478.

Snedecor, G.W. 1989. *Statistical Methods* 8th Edition. Iowa State University Press. 503 pp.

Souza, A. & Yang, Y. 2021. High-Throughput Corn Image Segmentation and Trait Extraction Using Chlorophyll Fluorescence Images. *Plant Phenomics* **2021**, Article ID 9792582, 15 pp.

Stirbet, A. & Govindjee. 2011. On the relation between the Kautsky effect (chlorophyll a fluorescence induction) and photosystem II: Basis and applications of the OJIP fluorescence transient. *Journal of Photochemistry and Photobiology B* **104**, 236–257.

Stirbet, A. & Govindjee. 2012. Chlorophyll a fluorescence induction: a personal perspective of the thermal phase, the J-I-P rise. *Photosynthesis Research* **113**, 15–61.

Stirbet, A., Lazár, D., Kromdijk, J. & Govindjee 2018. Chlorophyll a fluorescence induction: can just a one-second measurement be used to quantify abiotic stress responses? *Photosynthetica* **56**, 86–104.

Stirbet, A., Riznichenko, G.Y., Rubin, A.B. & Govindjee. 2014. Modeling chlorophyll a fluorescence transient: relation to photosynthesis. *Biochemistry-Moscow*+ **79**, 291–323.

Suárez, J.C., Vanegas, J.I., Contreras, A.T., Anzola, J.A., Urban, M.O., Beebe, S.E., Rao, I.M. 2022. Chlorophyll Fluorescence Imaging as a Tool for Evaluating Disease Resistance of Common Bean Lines in the Western Amazon Region of Colombia. *Plants* **11**, 1371.

Test Guidelines for the conduct of tests for distinctness. uniformity and stability of Fodder Radish (*Raphanus sativus* L. var. *oleiformis* Pers.). Geneva. 2017. 19 p.

Thach, L.B., Shapcott, A., Schmidt, S. & Critchley, C. 2007. The OJIP fast fluorescence rise characterizes Craptophyllum species and their stress responses. *Photosynthesis Research* (**94**)2, 423–436.

Tikkanen, M., Mekala, N.R. & Aro, E.M. 2014. Photosystem II photoinhibition-repair cycle protects photosystem I from irreversible damage. *Biochimica et Biophysica Acta* **1837**, 210–215.

Tomaškin, J., Tomaškinová, J. & Theuma, H. 2021. Chlorophyll Fluorescence as a Criterion for the Diagnosis of Abiotic Environmental Stress of Miscanthus x Giganteus Hybrid. *Polish Journal of Environmental Studies* **30**(4), 3269–3276.

Tsai, Y.C., Chen, K.C., Cheng, T.S., Lee, C., Lin, S.H. & Tung, C.W. 2019. Chlorophyll fluorescence analysis in diverse rice varieties reveals the positive correlation between the seedlings salt tolerance and photosynthetic efficiency. *MC Plant Biology* **19**, 403.

Tsytsiura, Y.H. 2019. Evaluation of the efficiency of oil radish agrophytocoenosis construction by the factor of reproductive effort. *Bulgarian Journal of Agricultural Science* **25**(6), 1161–1174.

Tsytsiura, Y.H. 2020. Modular-vitality and ideotypical approach in evaluating the efficiency of construction of oilseed radish agrophytocenosises (*Raphanus sativus* var. *oleifera* Pers.). *Agraarteadus* **31**(2), 219–243.

Tsytsiura, Y. 2020a. Formation and determination of the individual area of oilseed radish leaves in agrophytocenosises of different technological construction. *Agronomy Research* **18**(3), 2217–2244.

Tsytsiura, Ya.H. 2021. Matrix quality variability of oilseed radish (*Raphanus sativus* L. var. *oleiformis* Pers.) and features of its formation in technologically different construction of its agrophytocenosis. *Agronomy Research* **19**(1), 300–326.

Valcke, R. 2021. Can chlorophyll fluorescence imaging make the invisible visible? *Photosynthetica* **59**(SI), 381–398.

Van Zelm, E., Zhang, Y. & Testerink, C. 2020. Salt tolerance mechanisms of plants. *Annual Review of Plant Biology* **71**, 1–31.

Viljevac Vuleti´c, M., Mihaljevi´c, I., Tomaš, V., Horvat, D., Zduni´c, Z. & Vukovi´c, D. 2022. Physiological Response to Short-Term Heat Stress in the Leaves of Traditional and Modern Plum (*Prunus domestica* L.) Cultivars. *Horticulturae* **8**, 72.

Wang, S., Huang, C., Zhang, L., Lin, Y., Cen, Y. & Wu, T. 2016. Monitoring and assessing the 2012 drought in the Great Plains: Analyzing satellite-retrieved solar-induced chlorophyll fluorescence, drought indices, and gross primary production. *Remote Sensing* **8**, 61.

Wang, C., Gu, Q., Zhao, L., Li, C., Ren, J. & Zhang, J. 2022. Photochemical Efficiency of Photosystem II in Inverted Leaves of Soybean [*Glycine max* (L.) Merr.] Affected by Elevated Temperature and High Light. *Frontiers in Plant Science* **12**, 772644.

Żelazny, W.R. & Lukáš, J. 2020. Drought Stress Detection in Juvenile Oilseed Rape Using Hyperspectral Imaging with a Focus on Spectra Variability. *Remote Sensing* **12**(20), 3462.

Zhang, J., Zhao, B., Yang, C., Shi, Y., Liao, Q., Zhou, G., Wang, C., Xie, T., Jiang, Z., Zhang, D., Yang, W., Huang, C. & Xie, J 2020. Rapeseed Stand Count Estimation at Leaf Development Stages With UAV Imagery and Convolutional Neural Networks. *Frontiers in Plant Science* **11**, 617.